

TEXTE

40/2023

Final report

Bioaccumulation assessment of superhydrophobic substances

by:

Prof. Dr. Kai-Uwe Goss

Helmholtz Centre for Environmental Research GmbH - UFZ, Leipzig

Dr. Andrea Ebert

Helmholtz Centre for Environmental Research GmbH - UFZ, Leipzig

publisher:

German Environment Agency

TEXTE 40/2023

Ressortforschungsplan of the Federal Ministry for the
Environment, Nature Conservation, Nuclear Safety and
Consumer Protection

Project No. 157927

Report No. (UBA-FB) FB000851/ENG

Final report

Bioaccumulation assessment of superhydrophobic substances

by

Prof. Dr. Kai-Uwe Goss

Helmholtz Centre for Environmental Research GmbH -
UFZ, Leipzig

Dr. Andrea Ebert

Helmholtz Centre for Environmental Research GmbH -
UFZ, Leipzig

On behalf of the German Environment Agency

Imprint

Publisher

Umweltbundesamt
Wörlitzer Platz 1
06844 Dessau-Roßlau
Tel: +49 340-2103-0
Fax: +49 340-2103-2285
buergerservice@uba.de
Internet: www.umweltbundesamt.de

[f/umweltbundesamt.de](https://www.facebook.com/umweltbundesamt.de)

[t/umweltbundesamt](https://twitter.com/umweltbundesamt)

Report performed by:

Helmholtz Centre for Environmental Research GmbH - UFZ
Permoserstraße 15
04318 Leipzig
Germany

Report completed in:

April 2022

Edited by:

Section IV 2.3
Juliane Ackermann; Gabriele Treu

Publication as pdf:

<http://www.umweltbundesamt.de/publikationen>

ISSN 1862-4804

Dessau-Roßlau, March 2023

The responsibility for the content of this publication lies with the author(s).

Abstract: Bioaccumulation assessment of superhydrophobic substances

Bioconcentration tests with the freshwater amphipod *Hyaella azteca* (HYBIT) have been proposed as alternatives to fish tests, and the respective experimental BCF values show promising correlations. It is unclear whether the HYBIT test is also suitable for highly hydrophobic chemicals, such as UV stabilizers UV-234 and UV-329. In order to estimate the range in which the uptake rate constant k_1 would be expected for these substances, a prediction method for k_1 in *H. azteca* was developed in this work. As a result, we found that the experimental literature values appear plausible compared to the predicted values within the given uncertainties, however, more experimental data is needed for a conclusive validation. The main uncertainties for the prediction are the uncertainty of the determination of the octanol/water partition coefficient and the chemical's binding to organic matter in water (TOC).

Compared to fish tests, HYBIT seems promising for superhydrophobic substances, not only because of the experimental advantages such as smaller experimental units. According to the model, measurement (in the absence of metabolism) will benefit from a tendentially higher depuration rate constant k_2 in *H. azteca* than in fish, which would shorten the time to steady state. Nevertheless, for *H. azteca*, according to the modeling, the required times till steady state in the superhydrophobic range are to be expected far longer than standard test durations (up to months). However, the use of the BCF as an evaluation criterion for the bioaccumulation of superhydrophobic substances is conceptually questionable. For superhydrophobic substances, the introduction of feces as an additional elimination path, without the parallel intake of contaminated food as would be realistic, has the effect that even without metabolism or growth, the BCF values decrease with increasing K_{ow} , which would not be expected under real circumstances.

Kurzbeschreibung: Bioakkumulationsbewertung von superhydrophoben Stoffen

Biokonzentrationsstests mit dem Süßwasserflohkrebs *Hyaella azteca* (HYBIT) wurden als Alternative zu Fischtests vorgeschlagen, und die entsprechenden experimentellen BCF Werte zeigen vielversprechende Korrelationen. Ob der HYBIT-Test auch für stark hydrophobe Chemikalien wie die UV-Stabilisatoren UV-234 und UV-329 geeignet ist, ist unklar. Um abzuschätzen, in welchem Bereich die Aufnahmeratenkonstante k_1 für diese Substanzen zu erwarten wäre, wurde in dieser Arbeit ein Vorhersagemodell für k_1 in *H. azteca* entwickelt. Experimentelle Literaturwerte erscheinen im Rahmen der gegebenen Unsicherheiten gegenüber den vorhergesagten Werten plausibel, für eine abschließende Validierung sind jedoch weitere experimentelle Daten erforderlich. Die wichtigsten Unsicherheitsfaktoren für die Vorhersage sind die Unsicherheit der Bestimmung des Octanol/Wasser-Verteilungskoeffizienten und die Bindung der Chemikalie an organisches Material in Wasser (TOC).

Im Vergleich zu Fisch-Tests erscheint HYBIT für superhydrophobe Substanzen vielversprechend, nicht nur wegen der experimentellen Vorteile wie kleineren Versuchseinheiten. Dem Modell zufolge profitiert die Messung in *H. azteca* (ohne Metabolismus) von einer tendenziell höheren Depurationsratenkonstante k_2 als im Fisch, was die Zeit bis zum Steady State verkürzen sollte. Dennoch sind für *H. azteca* laut Modellierung im superhydrophoben Bereich Zeiten bis zum Steady State zu erwarten, die weit über den Standardtestzeiten (bis zu Monaten) liegen. Die Verwendung des BCF als Bewertungskriterium für die Bioakkumulation von superhydrophoben Stoffen ist jedoch grundsätzlich fragwürdig. Bei superhydrophoben Substanzen führt die Einführung von Kot als zusätzlichen Ausscheidungsweg, ohne die in der Realität damit gekoppelte Aufnahme kontaminierter Nahrung, dazu, dass auch ohne Metabolismus oder Wachstum die BCF-Werte mit steigendem K_{ow} sinken, was so nicht zu erwarten wäre unter realen Umständen.

Table of content

| | |
|---|----|
| List of figures | 8 |
| List of tables | 8 |
| List of abbreviations | 10 |
| Summary | 12 |
| Zusammenfassung..... | 14 |
| 1 Introduction..... | 17 |
| 2 Workpackage 1: k1 Model Development..... | 18 |
| 2.1 Physiological data..... | 18 |
| 2.1.1 Hyalella azteca | 18 |
| 2.1.1.1 Body composition | 18 |
| 2.1.1.2 Respiration rate and ventilation rate constant | 18 |
| 2.1.1.3 Food assimilation efficiencies..... | 19 |
| 2.1.1.4 Blood composition and volume..... | 19 |
| 2.1.1.5 Organ surface areas..... | 19 |
| 2.2 Compound specific data..... | 21 |
| 2.2.1 Compounds of interest | 21 |
| 2.2.2 Octanol/water partition coefficient and uncertainties in its prediction | 22 |
| 2.3 Fundamental processes | 23 |
| 2.3.1 Binding to TOC | 23 |
| 2.3.2 Diffusion..... | 25 |
| 2.3.2.1 Unstirred water layer..... | 25 |
| 2.3.2.2 Facilitated transport | 25 |
| 2.3.3 Cell permeation..... | 27 |
| 2.3.4 Bloodflow | 27 |
| 2.4 Identification of relevant uptake/elimination paths in Hyalella azteca..... | 27 |
| 2.4.1 Uptake/elimination via gills | 28 |
| 2.4.2 Uptake/elimination via gut | 29 |
| 2.4.3 Uptake/elimination via skin (deemed irrelevant)..... | 31 |
| 2.4.4 Elimination via metabolism | 31 |
| 2.5 Calculation of k1 and k2..... | 31 |
| 2.5.1 Resulting rate constants | 31 |
| 2.5.2 Comparison of modeled to experimental k1..... | 33 |
| 2.5.3 k1 depending on K_{ow} | 34 |

| | | |
|-------|--|----|
| 2.5.4 | Limits of applicability | 35 |
| 3 | Workpackage 2: Suitability of the Hyalella BCF test for superhydrophobic substances..... | 36 |
| 3.1 | Modeled k2 to estimate time till steady state | 36 |
| 3.2 | BCF | 38 |
| 3.3 | Comparability between BCF studies with fish and Hyalella azteca | 39 |
| 3.4 | Limits of applicability | 41 |
| 4 | List of references | 43 |
| A | Appendix..... | 46 |
| A.1 | DOC | 46 |
| A.2 | Facilitation factor in blood | 48 |
| A.3 | Bile acids as carriers in the gut..... | 50 |
| A.4 | Cell permeation..... | 51 |
| A.5 | Comparison of modeled rate constant k2 in H. azteca and fish | 52 |
| A.6 | Tabular data | 52 |

List of figures

| | | |
|------------|--|----|
| Figure 1: | UV-absorbers UV-234 and UV-329 | 21 |
| Figure 2: | Uncertainty in K_{ow} prediction | 22 |
| Figure 3: | Bioavailable fraction $f_{unbound}$ | 24 |
| Figure 4: | BCF if only uptake/elimination over gills is considered..... | 24 |
| Figure 5: | Facilitated transport | 26 |
| Figure 6: | Considered uptake and elimination paths | 28 |
| Figure 7: | Uptake and elimination via gills | 28 |
| Figure 8: | Importance of single resistances in gills..... | 29 |
| Figure 9: | Uptake and elimination via gut | 29 |
| Figure 10: | Importance of single resistances in gut..... | 31 |
| Figure 11: | Modeled and experimental k_1 | 33 |
| Figure 12: | Modeled k_1 depending on K_{ow} | 34 |
| Figure 13: | Modeled and experimental k_2 | 36 |
| Figure 14: | Modeled k_2 depending on K_{ow} | 37 |
| Figure 15: | Estimated t_{50} of depuration phase..... | 38 |
| Figure 16: | Contributions of $k_{2,gills}$ and k_E to k_2 | 38 |
| Figure 17: | Log BCF for (super)hydrophobic chemicals..... | 39 |
| Figure 18: | Log BCF in <i>Hyalella azteca</i> and in fish..... | 41 |
| Figure 19: | Influence of facilitated transport with DOC on log BCF | 48 |
| Figure 20: | Correlation between micelle facilitation factor and K_{ow} | 51 |
| Figure 21: | Comparison of modeled rate constant k_2 in <i>H. azteca</i> and fish | 52 |

List of tables

| | | |
|----------|--|----|
| Table 1: | Physiological data in <i>Hyalella azteca</i> and fish | 20 |
| Table 2: | SMILES, Molecular weight MW and log K_{ow} of hydrophobic chemicals | 21 |
| Table 3: | System of equations gills | 32 |
| Table 4: | System of equations gut..... | 32 |
| Table 5: | System of equations gills considering de-/sorption kinetics.... | 47 |
| Table 6: | System of equations considering de-/sorption kinetics to calculate FAC in blood | 49 |
| Table 7: | Diffusion coefficient D_w , albumin/water partition coefficient $K_{albumin/w}$, aqueous solubility S_w , melting temperature T_m , subcooled solubility $S_{subcooled}$, calculated facilitation factors by bile micelles in the gut FAC_{mic} and albumin in blood $FAC_{albumin}$ for hydrophobic chemicals | 52 |
| Table 8: | Calculated facilitation factors by bile micelles in the gut FAC_{mic} and albumin in blood $FAC_{albumin}$ depending on the octanol/water partition coefficient log K_{ow} | 53 |

| | |
|-----------|---|
| Table 9: | Predicted rate constants k_1 , k_2 (not considering metabolism), k_{2m} (considering metabolism), experimental rate constants k_{1exp} and k_{2exp} , predicted biotransformation half life54 |
| Table 10: | Calculated log BCF (without consideration of metabolism), log BCF_m (considering metabolism), BCF_{exp_k2} (calculated using calculated k_1 and experimental k_2), and experimental BCF_{exp} 54 |
| Table 11: | Hyalella Azteca: Calculated rate constants k_1 for TOC content of 1 mg DOC/L and 2 mg DOC/L, respectively, k_2 and estimated times till steady state, 50% and 90% respectively, depending on the octanol/water partition coefficient log K_{ow}55 |
| Table 12: | Fish: Calculated rate constants k_1 for TOC content of 1 mg DOC/L and 2 mg DOC/L, respectively, k_2 and estimated times till steady state, 50% and 90% respectively, depending on the octanol/water partition coefficient log K_{ow}56 |
| Table 13: | log BCF in H. Azteca and fish, calculated for 1 mg DOC/L and 2 mg DOC/L, respectively, depending on the octanol/water partition coefficient log K_{ow}57 |

List of abbreviations

| | |
|-------------------------------|---|
| ABL | aqueous boundary layer |
| A_{gills} | gill surface area |
| A_{gut} | gut surface area |
| A_{skin} | total body surface area |
| BCF | bioconcentration factor |
| BW | organism body weight |
| C_{L,org} | total lipid content of organism |
| C_{NLOM,org} | non lipid organic matter content of organism |
| C_{OX} | oxygen concentration in water |
| C_{W,org} | water content of organism |
| d | day |
| DOC | dissolved organic matter content in water |
| D_w | diffusion coefficient in water |
| ε_L | dietary assimilation rate of lipids |
| ε_N | dietary assimilation rate of NLOM |
| ε_w | dietary assimilation rate of water |
| FAC | facilitation factor |
| FAC_{albumin} | facilitation factor with albumin in blood as carrier |
| FAC_{mic} | facilitation factor with bile micelles in gut as carriers |
| f_{unbound} | unbound fraction |
| H. azteca | hyalella azteca |
| k₁ | uptake rate constant |
| k₂ | depuration rate constant |
| k_{2,gills} | elimination rate constant via gills |
| k_{2,gut} | elimination rate constant via gut |
| k_{2m} | predicted depuration rate constant considering metabolism |
| K_{alb/w} | albumin/water partition coefficient |
| k_{diet} | dietary uptake rate constant |
| kg_{org} | kilogram organism |
| k_{metabolism} | elimination rate constant via metabolism |
| K_{org/w} | organism/water partition coefficient |
| K_{ow} | octanol/water partition coefficient |
| k_{vent} | ventilation rate constant |
| L_w | liter water |
| MW | molecular weight |
| NLOM | non lipid organic matter |
| O₂ | oxygen |
| PCB153 | 2,2',4,4',5,5'-hexachloro-1,1'-biphenyl |
| PCB77 | 3,3',4,4'-tetrachlorobiphenyl |
| POC | particulate organic matter content in water |
| R | gas constant |
| SMILES | simplified molecular input line entry specification |

| | |
|------------------------------|---|
| ABL | aqueous boundary layer |
| S_{subcooled} | subcooled solubility |
| S_w | aqueous solubility |
| t50 | time till 50% of steady state is reached |
| t90 | time till 90% of steady state is reached |
| T_m | melting temperature |
| TOC | total organic matter content in water |
| UV-234 | 2-(2h-benzotriazol-2-yl)-4,6-bis(2-phenyl-2-propanyl)phenol |
| UV-329 | 2-(2h-benzotriazol-2-yl)-4-(1,1,3,3-tetramethylbutyl)phenol |

Summary

Bioconcentration tests with the freshwater amphipod *Hyaella azteca* (HYBIT) have been proposed as alternatives to fish tests, which is desirable in terms of reducing the number of vertebrates used for testing under the 3R principles of Replacement, Reduction and Refinement (de Wolf et al., 2007). The respective bioconcentration factors BCF show promising correlations. It is still unclear though whether HYBIT is also suitable for highly hydrophobic chemicals, such as UV stabilizers UV-234 and UV-329. These chemicals have been tested in *H. azteca* for their bioaccumulative potential (Schlechtriem et al., 2021), yet strong variations in the uptake rate constants k_1 were observed, not only between fish and *H. azteca*, but also between different experiments conducted in *H. azteca* for the same chemical. In *H. azteca*, k_1 for UV-329 ranged from 8 288 $L_w/kg_{org}/d$ to 66 085 L_w/kg_{org} . Yet, we believe the second value to be an experimental artefact due to the strong growth of biofilm, which might have led to the uptake of contaminated diet. It will therefore not be discussed any further. To assess whether the increased k_1 as compared to fish are realistic, we developed a model to predict k_1 from the K_{ow} and molecular weight MW in workpackage 1. In workpackage 2, we evaluated the suitability of HYBIT for superhydrophobic substances.

A detailed literature search was undertaken to gather the physiological data necessary for model development, and to determine the relevant uptake/elimination processes.

Data regarding the respiration rate and uptake efficiency of O_2 allowed the estimation of the ventilation rate constant, which resulted in quite similar values as estimated empirically for fish of the same weight. Empirical correlations developed for amphipods were used, or physiological data from similar amphipods were scaled down to estimate organ surface areas. Estimates for unstirred water layer thickness in water and blood correspond to assumptions made in literature, in case of blood assumed for fish. Although data on protein content in amphipods exist, binding kinetics and partition coefficients are yet unknown. For the calculations, we thus assumed proteins similar to albumin in fish, which might act as a carrier across the unstirred layer in blood for superhydrophobic compounds and thus facilitate transport. Having no data on bloodflow in *H. azteca*, we simply assumed it to be insignificant for superhydrophobic chemicals due to facilitated transport by the albumin-like protein. We also collected information on the test chemicals UV-234 and UV-329. Predicted octanol/water partition coefficients varied widely between different prediction methods, resulting in a broad uncertainty in k_1 prediction. We decided to use the mean $\log K_{ow}$ for calculations.

The physiological data allowed the determination of relevant uptake processes:

The amphipods were fed uncontaminated diet, therefore the diet was excluded as a possible uptake path. We had a closer look at uptake via skin, because the area to volume ratio is higher for smaller animals. Yet, the total body area was estimated to be only marginally higher than gill area. Taking into account the chitin shell, additional cell layers, and an increased unstirred water layer as compared to the gills, this possible uptake path was deemed irrelevant. We thus identified uptake via gills as the important uptake path. For the uptake via gills, another effect must be considered. The influence of chemical binding to organic matter (TOC) in water is very high for superhydrophobic chemicals. The bioavailable fraction may decrease by orders of magnitude, decreasing k_1 in turn. It is not yet clear whether for superhydrophobic chemicals, some fraction of chemical bound to TOC might still be bioavailable, i.e. whether de-/sorption kinetics are fast enough for the chemical to diffuse across the ventilation volume or unstirred water layer bound to TOC and then desorb before being absorbed by the gills. Yet, we assumed

all chemical bound to TOC as not-bioavailable, which is the usual approach (Arnot and Gobas, 2004) (Arnot and Gobas, 2004), see section 2.3.1 for a detailed discussion.

Modeling k_1 revealed the unstirred layer in water and the ventilation rate as the main resistances for the uptake via gills. Within uncertainties, modeled k_1 values corresponded well to experimental values from literature, except for a slight overestimation of k_1 for chemicals with $\log K_{ow}$ below 6.5, which could be due to the absence of bloodflow in our modelling, which might be a limiting factor for low K_{ow} .

The resulting k_1 are indeed higher than expected for fish, due to the increased ventilation rate per body weight in *H. azteca*. Yet, we believe the extremely low k_1 value measured in fish for UV-329 to be an experimental artefact. There were problems maintaining solute concentration, resulting in an extreme intermediate drop in internal body concentration. Also, steady state was never reached, and the value lies well below predicted k_1 for fish. We thus conclude that experimentally measured k_1 in *Hyaella azteca* are quite plausible. Yet, data in the superhydrophobic range are too sparse and K_{ow} uncertainties too high to conclusively validate the prediction method or the experimental data.

In workpackage 2, we assessed the suitability of the BCF test in *H. azteca* for superhydrophobic substances. To this end, we estimated the elimination rate constant k_2 in HYBIT, which can be used to estimate the time till steady state is reached. To this end, feces was modeled as a further relevant elimination path besides the elimination via the gills. This elimination path gains more importance the higher the $\log K_{ow}$, and is dominant for superhydrophobic compounds. Resulting times till steady state (in the absence of metabolism or growth) were exceeding months for $\log K_{ow} > 7$, which is much longer than practicable for standard testing. Neither PCB153 ($\log K_{ow}$ 7.8, practically inert (Trowell et al., 2018)) nor PCB77 ($\log K_{ow}$ 6.7) reached steady state within 12 days of measurement (Schlechtriem et al., 2019).

Predicted BCF (in the absence of metabolism) in *H. azteca* and fish correlated well, similar to experimental results for lower $\log K_{ow}$ (Schlechtriem et al., 2019). Yet, both experimental and modeled k_2 (and k_1) were higher in *Hyaella azteca* than in fish, which is an advantage due to shorter times till steady state. Due to the sparsity of data in the superhydrophobic range, and probably dominating metabolism in UV-234, a conclusive validation of the k_2 and BCF modeling was not possible in that range.

Overall, the BCF test in *H. azteca* might be more suitable for testing (super)hydrophobic compounds than conventional fish tests, but it will still be limited by the required duration of the experiments. However, more experimental data in the superhydrophobic range will be necessary to validate the method and identify its exact applicability domain.

There is also a general problem with the BCF for superhydrophobic compounds per se: By feeding an uncontaminated diet, an unrealistic additional elimination path is introduced, which would in reality always be accompanied by an uptake of contaminated food. As a result, BCF decrease with high $\log K_{ow}$, and chemicals may be classified as less bioaccumulative than chemicals with lower $\log K_{ow}$ (or not bioaccumulative at all), even in the absence of metabolism and even if the experiments are conducted flawlessly.

Zusammenfassung

Biokonzentrationstests mit dem Süßwasserflohkrebs *Hyalella azteca* (HYBIT) wurden als Alternative zu Fischtests vorgeschlagen, was wünschenswert ist, um die Anzahl der Wirbeltiere zu reduzieren, die für Tests gemäß den 3R-Prinzipien von Replacement, Reduction und Refinement verwendet werden (de Wolf et al., 2007). Die jeweiligen Biokonzentrationsfaktoren BCF zeigen vielversprechende Korrelationen. Ob HYBIT auch für stark hydrophobe Chemikalien wie die UV-Stabilisatoren UV-234 und UV-329 geeignet ist, ist unklar. Diese Chemikalien wurden in *H. azteca* auf ihr Bioakkumulationspotenzial getestet (Schlechtriem et al., 2021), jedoch wurden starke Unterschiede in den Aufnahmeratenkonstante k_1 beobachtet, nicht nur zwischen Fischen und *H. azteca*, sondern auch zwischen verschiedenen durchgeführten Experimenten mit *H. azteca* für die gleiche Chemikalie. Bei *H. azteca* reichte k_1 für UV-329 von $8.288 \text{ L}_w/\text{kg}_{\text{org}}/\text{d}$ bis $66.085 \text{ L}_w/\text{kg}_{\text{org}}$. Wir halten den zweiten Wert jedoch für ein experimentelles Artefakt aufgrund eines starken Biofilmwachstums, der zur Aufnahme von kontaminierter Nahrung geführt haben könnte. Es wird daher nicht weiter darauf eingegangen. Um zu beurteilen, ob die erhöhten k_1 im Vergleich zu Fischen realistisch sind, haben wir in Arbeitspaket 1 ein Modell zur Vorhersage von k_1 aus K_{ow} und Molekulargewicht MW entwickelt. In Arbeitspaket 2 haben wir die Eignung von HYBIT für superhydrophobe Substanzen bewertet.

Eine ausführliche Literaturrecherche wurde durchgeführt, um die für die Modellentwicklung erforderlichen physiologischen Daten zu sammeln und die relevanten Aufnahme-/Eliminationsprozesse zu bestimmen.

Daten zur Respirationsrate und Aufnahmeeffizienz von O_2 ermöglichten die Abschätzung der Ventilationsrate, was zu ziemlich ähnlichen Werten führte, wie sie empirisch für Fische mit gleichem Gewicht geschätzt werden. Für Amphipoden entwickelte empirische Korrelationen wurden verwendet, oder physiologische Daten von ähnlichen Amphipoden wurden herunterskaliert, um die Organoberflächen abzuschätzen. Abschätzungen für die ungerührte Wasserschichtdicke in Wasser und Blut entsprechen Annahmen aus der Literatur, im Falle von Blut basierte der Wert auf Annahmen im Fisch. Obwohl Daten zum Proteingehalt in Amphipoden existieren, sind Bindungskinetik und Verteilungskoeffizienten noch unbekannt. Für die Berechnungen haben wir daher ein dem Albumin in Fischen ähnliches Protein angenommen, das für superhydrophobe Verbindungen als Carrier durch die ungerührte Schicht im Blut fungieren und so den Transport erleichtern könnte. Da wir keine Daten zum Blutfluss in *H. Azteka* hatten, nahmen wir an, dass er (als Diffusionsbarriere) für superhydrophobe Chemikalien aufgrund des facilitated Transports durch das albuminähnliche Protein unbedeutend ist. Es wurden auch Informationen zu den Testchemikalien UV-234 und UV-329 gesammelt. Die vorhergesagten Oktanol/Wasser-Verteilungskoeffizienten variierten stark zwischen den verschiedenen Vorhersagemethoden, was zu einer großen Unsicherheit bei der k_1 -Vorhersage führte. Wir haben daher für die Berechnungen den mittleren $\log K_{ow}$ verwendet.

Die physiologischen Daten erlaubten die Bestimmung der relevanten Aufnahmeprozesse: Die Amphipoden wurden mit unkontaminierter Nahrung gefüttert, daher wurde die Nahrung als möglicher Aufnahmeweg ausgeschlossen. Die Aufnahme über die Haut wurde genauer betrachtet, da das Flächen-zu-Volumen-Verhältnis bei kleineren Tieren höher ist. Die Gesamtkörperfläche wurde jedoch nur um einen kleinen Faktor größer als die Kiemenfläche geschätzt. Unter Berücksichtigung des Chitinpanzers, zusätzlicher Zellschichten und einer gegenüber den Kiemen erhöhten ungerührten Wasserschicht wurde dieser mögliche Aufnahmepfad als irrelevant erachtet. Wir identifizierten daher die Aufnahme über Kiemen als wichtigsten Aufnahmeweg. Bei der Aufnahme über die Kiemen muss ein weiterer Effekt berücksichtigt werden. Der Einfluss der Bindung an organische Stoffe (TOC) im Wasser ist bei

superhydrophoben Chemikalien sehr hoch. Die bioverfügbare Fraktion kann um Größenordnungen abnehmen, was wiederum k_1 verringert. Es ist noch unklar, ob bei superhydrophoben Chemikalien eine an TOC gebundene Chemikalie möglicherweise noch teilweise bioverfügbar ist, d.h. ob die De-/Sorptionskinetik schnell genug ist, damit die Chemikalie durch das Ventilationsvolumen oder die ungerührte Wasserschicht, die an TOC gebunden ist, diffundieren, dann desorbieren und von den Kiemen aufgenommen werden kann. Wir haben jedoch angenommen, dass alle an TOC gebundenen Chemikalien nicht bioverfügbar sind, was der übliche Ansatz ist (Arnot and Gobas, 2004), siehe Sektion 2.3.1 für eine ausführliche Diskussion.

Die Modellierung von k_1 ergab die ungerührte Wasserschicht und die Ventilationsrate als Hauptwiderstände für die Aufnahme über die Kiemen. Innerhalb von Unsicherheiten entsprachen die modellierten k_1 -Werte gut den experimentellen Werten aus der Literatur, mit Ausnahme einer leichten Überschätzung von k_1 für Chemikalien mit $\log K_{ow}$ unter 6,5, was auf das Fehlen von Blutfluss in unserer Modellierung zurückzuführen sein könnte, der ein limitierender Faktor für niedrige K_{ow} sein könnte. Die resultierenden k_1 sind in der Tat höher als für Fische erwartet, aufgrund der erhöhten Ventilationsrate pro Körpergewicht bei *H. azteca*. Wir glauben jedoch, dass der extrem niedrige k_1 -Wert, der in Fischen für UV-329 gemessen wurde, ein experimentelles Artefakt ist. Es gab Probleme, die Konzentration der Chemikalie in Wasser aufrechtzuerhalten, was zu einem extremen intermediären Abfall der Konzentration im Inneren des Organismus führte. Außerdem wurde der Steady State nie erreicht, und der Wert liegt deutlich unter dem vorhergesagten k_1 für Fische.

Wir schließen daraus, dass die experimentell gemessenen k_1 in *Hyaella azteca* ziemlich plausibel sind. Allerdings sind die existierenden Daten im superhydrophoben Bereich insgesamt zu spärlich und die K_{ow} -Unsicherheiten zu hoch, um die Vorhersagemethode oder die experimentellen Daten abschließend zu validieren.

In Arbeitspaket 2 haben wir die Eignung des BCF-Tests in *H. Azteca* für superhydrophobe Substanzen bewertet. Daher haben wir die Eliminationsratenkonstante k_2 in HYBIT geschätzt, die verwendet werden kann, um die Zeit abzuschätzen, bis ein stationärer Zustand erreicht ist. Dazu wurde neben der Ausscheidung über die Kiemen der Kot als weiterer relevanter Ausscheidungsweg modelliert. Dieser Eliminationsweg gewinnt mit zunehmendem $\log K_{ow}$ an Bedeutung und ist für superhydrophobe Verbindungen der dominierende. Die resultierenden Zeiten bis zum Steady State (ohne Metabolismus oder Wachstum) überstiegen Monate für $\log K_{ow} > 7$, was viel länger ist, als für Standardtests praktikabel. Weder PCB153 ($\log K_{ow}$ 7,8, praktisch inert (Trowell et al., 2018)) noch PCB77 ($\log K_{ow}$ 6,7) erreichten innerhalb von 12 Tagen nach der Messung den Steady State (Schlechtriem et al., 2019). Der vorhergesagte BCF (in Abwesenheit von Metabolismus) in *H. Azteca* und Fisch korrelierte gut, ähnlich wie experimentelle Ergebnisse für niedrigeres $\log K_{ow}$ (Schlechtriem et al., 2019). Dennoch waren sowohl experimentelle als auch modellierte k_2 (und k_1) bei *Hyaella azteca* höher als bei Fisch, was aufgrund der kürzeren Zeiten bis zum Steady State ein Vorteil ist. Aufgrund der wenigen Daten im superhydrophoben Bereich und des wahrscheinlich dominierenden Metabolismus in UV-234 war eine abschließende Validierung der k_2 - und BCF-Modellierung in diesem Bereich nicht möglich. Insgesamt könnte der BCF-Test in *H. Azteca* besser geeignet sein, um (super)hydrophobe Verbindungen zu testen als herkömmliche Fischtests, aber er sollte immer noch durch die erforderliche Dauer der Experimente begrenzt sein. Es sind jedoch weitere experimentelle Daten im superhydrophoben Bereich erforderlich, um die Methode zu validieren und ihren genauen Anwendungsbereich zu identifizieren.

Auch beim BCF für superhydrophobe Verbindungen per se gibt es ein generelles Problem: Durch die Fütterung mit unkontaminierter Nahrung wird ein unrealistischer zusätzlicher

Ausscheidungspfad eingeführt, der in Wirklichkeit immer mit einer Aufnahme kontaminierter Nahrung einhergehen würde. Infolgedessen nimmt der BCF mit hohem $\log K_{ow}$ ab, und Chemikalien könnten im Extremfall als weniger bioakkumulativ als Chemikalien mit niedrigerem $\log K_{ow}$ (oder überhaupt nicht bioakkumulativ) eingestuft werden, selbst wenn kein Metabolismus stattfindet.

1 Introduction

There is well-founded hope that in the future many fish bioaccumulation studies can be replaced by corresponding studies with *Hyalella azteca*. This is a desirable development in terms of reducing the number of vertebrates used for testing. However, it must be ensured that the informative value of these tests is comparable to the classic studies according to OECD 305. Superhydrophobic substances ($\log K_{ow} > 8$) cannot be tested easily in the classic fish tests, because constant and controlled exposure via the water is difficult to achieve and because the absorption kinetics are very slow (it might take months to reach a steady state). Nevertheless, a relevant bioaccumulation can occur even with slow uptake. For fish, this is shown not only by experimental studies but also by toxicokinetic models which are in good agreement with the experimental studies. In view of this situation, it is of particular interest to understand whether the alternative determination of BCF with *Hyalella azteca* is suitable also for very hydrophobic substances. On the one hand, as with the fish BCF studies, experimental problems in ensuring a constant water concentration during exposure must be dealt with. Sorption of chemicals to organic matter (TOC, total organic carbon) within the culture medium can extremely reduce the available free aqueous concentration of superhydrophobic compounds (Burkhard, 2000; Böhm *et al.*, 2016). It is also important to find out whether the necessary uptake period (uptake studies that run over a period of months cannot be carried out in a standard test) speaks for the feasibility of the studies. The question of whether the uptake and distribution mechanisms of superhydrophobic substances are still comparable between *Hyalella azteca* and fish as test species must also be investigated. In the publication Larisch *et al.* (Larisch and Goss, 2018a), we were able to show that the uptake kinetics and internal distribution of superhydrophobic substances in fish essentially depend on the so-called "facilitated transport". In this process, the substances can use a shuttle mechanism to overcome aqueous boundary layers which would otherwise act as practically insurmountable barriers to absorption. Uncertainties regarding the uptake kinetics of hydrophobic substances in *Hyalella azteca* are also fed by the results of an UBA project (FKZ 3718 67 401 0), in which extreme fluctuations in the experimental k_1 values occurred, a fact that does not appear to be mechanistically easy to explain. This results in the following tasks for the project:

- 1) Development of a toxicokinetic model of the uptake of (super) hydrophobic substances in *Hyalella azteca* (k_1 method development).
- 2) Assessment of the suitability of the *Hyalella azteca* BCF test for superhydrophobic substances in view of the modeling results and the experience gained from the UBA project (FKZ 3718 67 401 0).

2 Workpackage 1: k1 Model Development

2.1 Physiological data

An extended literature search has been undertaken to collect the necessary physiological data on *Hyalella azteca* to allow for physiologically based modeling of k_1 , k_2 and BCF. In many cases, data have been extrapolated from other amphipods, or in the absence of sufficient data, some data were adopted from fish.

To give an overview, at the end of this section both physiological data on *Hyalella azteca* and fish are listed side by side in tabular form.

2.1.1 *Hyalella azteca*

2.1.1.1 Body composition

Model calculations were done with male *Hyalella azteca* of a mean wet weight of 3 mg and 2% lipid content, as preferred by (Schlechtriem et al., 2019). According to (Othman and Pascoe, 2001), this corresponds to about a body length of 4.5 mm, and a dry weight of 0.8 mg (read from Fig. 1 and 2). Water content of the organism was estimated to be 2.2 mg, subtracting the dry weight from the wet weight, which corresponds to 73% of the wet weight. Taking into account the 2% lipid content, NLOM (Non Lipid Organic Matter) content was assumed to be 25%.

2.1.1.2 Respiration rate and ventilation rate constant

The ventilation rate constant was calculated from experimentally determined respiration rates from literature. We found respiration rates for *H. azteca* of 1.3 mg O₂/g_{wetweight}/h (Everitt et al., 2020) at 23°C, 45 μL O₂/g_{dryweight}/min (Johnke, 1973) (with oxygen density of 1.1g/L and relation dry weight to wet weight of 0.8/3, this corresponds to 0.8 mg O₂/g_{wetweight}/h) at 25°C, and 205 mg O₂/g_{wetweight}/h (Gauthier et al., 2016). We used a value of 1 mg O₂/g_{wetweight}/h for the calculations, not considering the value of (Gauthier et al., 2016), because it exceeded the other values by more than a factor of 100.

We assumed an extraction efficiency for oxygen by the gills of 10%, as a few to 10% efficiency are typical for filter feeders, non-filter-feeding burrow-dwelling invertebrates, and some crustaceans (Barker Jørgensen et al., 1986). The experiments to be modeled were done at 23±3°C, with an oxygen concentration C_{OX} between 6.9 and 9.3 mg/L (Schlechtriem et al., 2019). If not stated otherwise, we used 8 mg/L for the calculations.

The ventilation rate constant k_{vent} was then calculated as follows:

$$k_{vent} = \frac{\text{Respiratory rate}}{C_{OX} * \text{extraction efficiency}} \quad (1)$$

The resulting k_{vent} is 3*10⁴ L_w/kg_{org}/d. If not explicitly stated otherwise, we will refer in the following to wet weight if only weight is mentioned.

The result is quite similar to k_{vent} expected for a 3 mg fish estimated according to (Arnot and Gobas, 2004) using the empirical correlation of Equation (2), which results in 2*10⁴ L_w/kg_{org}/d:

$$k_{vent} = \frac{1400 * BW^{-0.35}}{C_{OX}} \quad (2)$$

Where BW is the weight of the organism in kg, and C_{OX} the oxygen concentration in mg O₂/L_w.

2.1.1.3 Food assimilation efficiencies

Food assimilation efficiencies in the gut for aquatic invertebrates were taken from (Arnot and Gobas, 2004), with a dietary assimilation rate of lipids of 75%, a dietary assimilation rate of NLOMs of 75%, and a dietary assimilation rate of water of 25%. These values will be needed to calculate the rate constant for elimination of the chemical through excretion of contaminated feces, see Section 2.4.2.

2.1.1.4 Blood composition and volume

Although there have been many studies on the protein composition of the hemolymph in the subphylum of crustaceans (Lorenzon et al., 2011; Fredrick and Ravichandran, 2012), protein contents in the hemolymph show wide interspecific variations (Rameshkumar et al., 2009), and we were not able to find information on the specific hemolymph protein content of *Hyalella azteca*. Blood composition is quite different in crustaceans than in fish, e.g. the blood contains no albumin (Depledge and Bjerregaard, 1989) or hemoglobin (Fredrick and Ravichandran, 2012). Yet, the protein hemocyanin transporting oxygen has a similar respiratory function as hemoglobin. It seems likely that there should also exist proteins equivalent to albumin that bind water-insoluble substances. In ignorance of the specific protein content, the partition coefficient and binding kinetics to these proteins, we will therefore assume an albumin-like protein in the hemolymph, and use the albumin content in fish, the albumin partition coefficient, and albumin binding kinetics for the calculations. Thus the diffusion coefficient of the albumin-like protein in water is assumed equal to that of albumin $6.3 \cdot 10^{-7} \text{ cm}^2/\text{s}$ (Gaigalas et al., 1992). We assume the same aqueous boundary layer (ABL) thickness in blood as for fish, 286 nm (Larisch and Goss, 2018b).

We will also assume a total blood volume of 30% of body weight, as was found for crustaceans *C. maenas* (Depledge and Bjerregaard, 1989).

2.1.1.5 Organ surface areas

Surface areas are critical values for our calculations, because diffusion across membranes or unstirred water layers is directly proportional to the area. This concerns especially the gills, gut and skin as possible uptake paths of the chemical.

2.1.1.5.1 Gills

To estimate the gill surface area A_{gills} , we used an empirical correlation developed for *Gammarus fossarum*, which like *Hyalella azteca* belongs to the order of amphipods (SUTCLIFFE, 1984):

$$A_{gills} = 5.4223 * BW_{dry}^{0.79} \quad (3)$$

Where BW_{dry} is the dry weight of the organism in mg. With a dry weight of 0.8 mg, we calculated a surface area of 0.05 cm^2 .

The unstirred water layer was estimated to be 5-8 μm in *Gammarus fossarum* (SUTCLIFFE, 1984), we will assume a value of 5 μm for *Hyalella azteca*.

2.1.1.5.2 Gut

For *Gammarus pulex*, the gut was reported as of cylindrical shape with a diameter of 0.28-0.6 mm for animals of 10-15 mm length (Welton et al., 1983). Scaling down to a bodylength of 4.5 mm for *Hyalella azteca*, this amounts to a diameter of about 0.2 mm. The surface area of a cylinder of diameter 0.2 mm and length of approximately 4.5 mm amounts to $9.6 \cdot 10^{-3} \text{ cm}^2$. Taking into account the presence of microvilli in the gut (Halcrow, 2001), we multiply by a factor

of 7.5 as is done for fish (Larisch and Goss, 2018b). The final calculated gut surface area is therefore $7.2 \cdot 10^{-2} \text{ cm}^2$.

2.1.1.5.3 Skin

Total body surface area A_{skin} was roughly estimated, approximating the organism by a cylindrical shape of length 4.5 mm. Calculated with a density of 1 kg/L, the BW of 3 mg corresponds to a volume of 3 mm³, and thus a cylindrical radius of 0.46 mm. This results in a total body surface area of 0.14 cm².

Table 1: Physiological data in *Hyalella azteca* and fish

| | <i>Hyalella azteca</i> | Fish ^a |
|--|---|---|
| Body composition | | |
| Wet weight | 3 mg | 2.2 g |
| Dry weight | 0.8 mg | |
| Body length | 4.5 mm | |
| Lipid content organism $C_{L,org}$ | 0.02 kg _{lipid} /kg _{org} | 0.02 kg _{lipid} /kg _{org} |
| Non Lipid Organic Matter content organism $C_{NLOM,org}$ | 0.25 kg _{NLOM} /kg _{org} | 0.19 kg _{NLOM} /kg _{org} |
| Water content organism $C_{W,org}$ | 0.73 kg _w /kg _{org} | 0.79 kg _w /kg _{org} |
| Respiration | | |
| Respiration rate | 1 mg O ₂ /g _{wetweight} /h | |
| Co _x | 8 mg O ₂ /L _w | 11 mg O ₂ /L _w |
| temperature | 23±3°C | 13°C |
| Ventilation rate constant | $3 \cdot 10^4 \text{ L}_w/\text{kg}_{org}/\text{d}$ | $2 \cdot 10^3 \text{ L}_w/\text{kg}_{org}/\text{d}$ |
| Food assimilation efficiencies | | |
| dietary assimilation rate of lipids ε_L | 75% | 92% |
| dietary assimilation rate of NLOM ε_N | 75% | 60% |
| dietary assimilation rate of water ε_W | 25% | 25% |
| Blood | | |
| Albumin(like) protein concentration | 41.2 g / L _{plasma} ^b | 41.2 g / L _{plasma} ^b |
| Blood volume/body weight | 30% | 6% |
| Organ surface areas | | |
| A_{gills} | 0.05 cm ² | 7 cm ² |
| A_{gut} | 0.07 cm ² | 3.8 cm ² |
| A_{skin} | 0.14 cm ² | 17 cm ² |

^a Values are calculated for rainbow trout of 2.2g at 13°C, as experimentally used in <https://echa.europa.eu/de/registration-dossier/-/registered-dossier/11135/5/4/2/?documentUUId=617b9e9b-a098-4a72-ad57-5cc5d53deed8>, k_{vent} was calculated as described in (Arnot and Gobas, 2004), assimilation rates were taken from (Arnot and Gobas, 2004), $A_{\text{gut}}/\text{kg}_{org}$ was taken

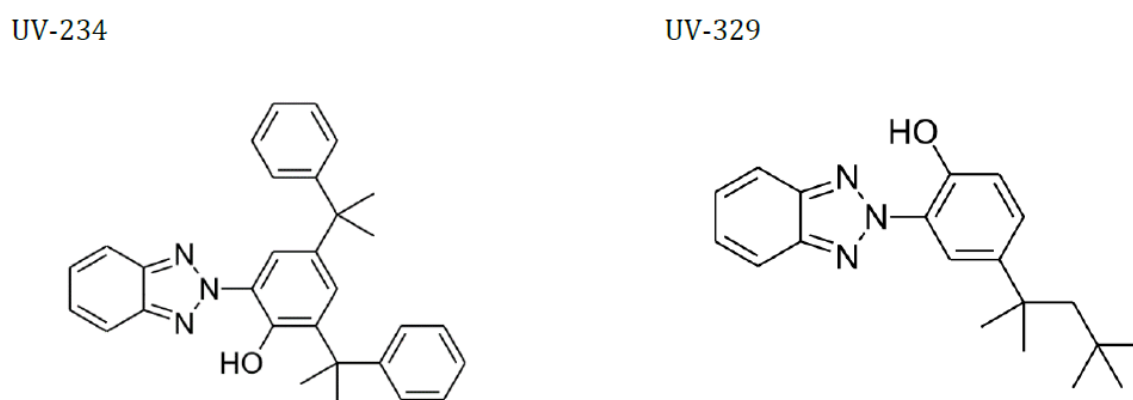
from (Buddington and Diamond, 1987), and multiplied by 7.5 to account for microvilli (Larisch and Goss, 2018b), A_{gills} was taken from (Morgan, 1971), A_{skin} was estimated from body weight $A_{skin}/cm^2=10*(BW/g)^{0.65}$ (Nichols et al., 1996), ^b from (Escher et al., 2011), assuming a protein density of 1.39 kg/L, this corresponds to $0.0296 L_{albumin}/L_{plasma}$.

2.2 Compound specific data

2.2.1 Compounds of interest

The UV-absorbers UV-234 and UV-329 (see Figure 1 for depiction of chemical structure) will be central to model development and validation, due to their superhydrophobic nature, and because experimental uptake/depletion data are available both in *Hyalella azteca* (Schlechtriem *et al.*, 2021) and fish (REACH registration dossier UV-329. <https://echa.europa.eu/de/registration-dossier/-/registered-dossier/13220/5/4/2/?documentUUID=e0ac66f4-ba8f-461a-aaeb-0cd0f9f85aa2>. REACH registration dossier UV-234. <https://echa.europa.eu/de/registration-dossier/-/registered-dossier/11135/5/4/2/?documentUUID=617b9e9b-a098-4a72-ad57-5cc5d53deed8>).

Figure 1: UV-absorbers UV-234 and UV-329



Chemical structures of the UV-absorbers UV-234 and UV-329

Source: own illustration, Helmholtz Centre for Environmental Research GmbH - UFZ

The developed k_1 model will also be tested against further hydrophobic compounds measured in *Hyalella azteca* (Schlechtriem *et al.*, 2019), see Table 2.

Table 2: SMILES, Molecular weight MW and log K_{ow} of hydrophobic chemicals

| Chemical | SMILES | MW (g/mol) | Log K_{ow} |
|-------------------|---|------------|--------------------------|
| UV-234 | <chem>CC(C)(c1ccccc1)c(cc1C(C)(C)c2ccccc2)cc(c1O)n1nc2ccccc2n1</chem> | 447.6 | 7.29 - 9.84 ^a |
| UV-329 | <chem>CC(C)(C)CC(C)(C)c(ccc1O)cc1n1nc2ccccc2n1</chem> | 323.4 | 6.5 - 7.29 ^a |
| hexachlorobenzene | <chem>C1(=C(C(=C(C(=C1Cl)Cl)Cl)Cl)Cl)Cl</chem> | 284.8 | 5.73 ^b |
| ortho-terphenyl | <chem>C1=CC=C(C=C1)C2=CC=CC=C2C3=CC=CC=C3</chem> | 230.3 | 5.75 ^b |
| benzo(a)pyrene | <chem>C1=CC=C2C3=C4C(=CC2=C1)C=CC5=C4C(=CC=C5)C=C3</chem> | 252.3 | 6.13 ^c |
| PCB153 | <chem>C1=C(C(=CC(=C1Cl)Cl)Cl)C2=CC(=C(C=C2Cl)Cl)Cl</chem> | 360.9 | 7.75 ^b |
| PCB77 | <chem>C1=CC(=C(C=C1C2=CC(=C(C=C2)Cl)Cl)Cl)Cl</chem> | 292.0 | 6.72 ^b |
| chlorpyrifos | <chem>CCOP(=S)(OCC)OC1=NC(=C(C=C1Cl)Cl)Cl</chem> | 350.57 | 4.96 ^d |

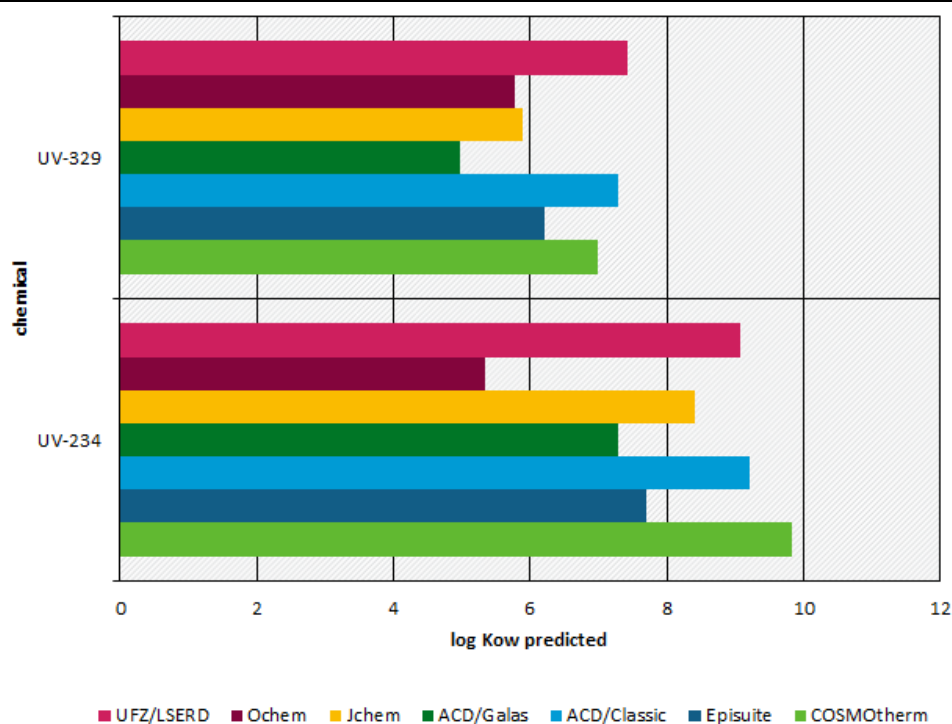
| Chemical | SMILES | MW (g/mol) | Log K _{ow} |
|--------------|---|------------|---------------------|
| methoxychlor | <chem>COC1=CC=C(C=C1)C(C2=CC=C(C=C2)OC)C(Cl)(Cl)Cl</chem> | 345.6 | 5.08 ^b |
| pyrene | <chem>C1=CC2=C3C(=C1)C=CC4=CC=CC(=C43)C=C2</chem> | 202.3 | 4.88 ^b |

^a predicted, ^b experimental (Hansch *et al.*, 1995), ^c experimental (De Maagd *et al.*, 1998), ^d J. Sangster: LogK_{ow} databank, version Jan. 1994

2.2.2 Octanol/water partition coefficient and uncertainties in its prediction

Several parameters are necessary for k1 model development. The most central input parameters are equilibrium partition coefficients. For simplicity, the octanol/water partition coefficient K_{ow} is used as a surrogate here. If available, experimental log K_{ow} are used, yet for superhydrophobic compounds, their determination can be tricky. In the case of UV-234 and UV-329 thus only lower limits of log K_{ow}=6.5 were measured. Various estimation tools agree on the high hydrophobicity, but large differences between the single estimations demonstrate the strong uncertainties in the predictions, see Figure 2. Some prediction tools may be outside their domain of applicability, although only Ochem (Sushko *et al.*, 2011) stated this clearly. As the bulk of correlations used here depend on the K_{ow}, this uncertainty will propagate into k1 predictions.

Figure 2: Uncertainty in K_{ow} prediction



Octanol/water partition coefficients predicted using different prediction tools, for UV-329 and UV-234. Predictions were done with COSMOtherm (COSMOtherm, Release 18. COSMOlogic, GmbH & Co. KG, Leverkusen, Germany. <http://www.cosmologic.de>.) (Eckert and Klamt, 2002), ACD/classics and ACD/Galas (ACD Percepta (2015 Release)), KOWWIN in EPI-SUITE (EPI-Suite. US EPA Estimation Programs Interface Suite™ for Microsoft® Windows, v 411. (<https://www.epa.gov/tsc-screening-tools/epi-suitetm-estimation-program-interface>)) (United States Environmental Protection Agency, 2012)), JChem for Excel (ChemAxon. JChem for Excel v. 20.6.0.618. <https://chemaxon.com/> (2020).), Ochem (Sushko *et al.*, 2011), or UFZ LSERD (Ulrich *et al.*, 2017).

Source: own illustration, Helmholtz Centre for Environmental Research GmbH - UFZ

Calculating the mean and standard deviation (not considering Ochem, which is out of its applicability domain), the log K_{ow} of UV-234 is 8.6 ± 0.9 , and log K_{ow} of UV-329 is 6.5 ± 0.9 .

2.3 Fundamental processes

2.3.1 Binding to TOC

Superhydrophobic compounds may bind to organic matter, particulate (POC) or dissolved (DOC) in water. Typical DOC values in drinking water are about 1 mg DOC / L_w , and the OECD Guideline 305 allows for a maximum total organic carbon content (TOC=POC+DOC) of 2 mg/ L_w . The stronger the chemical binds to TOC, and the higher the TOC content, the lower the actual bioavailable chemical fraction in water will be. This unbound fraction $f_{unbound}$ can be estimated according to (Burkhard, 2000):

$$f_{unbound} = 1 / (1 + C_{POC} * 0.35 * K_{ow} + C_{DOC} * 0.08 * K_{ow}) \quad (4)$$

Where C_{DOC} is the concentration of DOC in water in kg DOC/ L_w and C_{POC} is the concentration of POC in water in kg POC/ L_w .

It is unclear whether some of the fraction bound to TOC is still bioavailable (Erickson and McKim, 1990), because in case of high enough sorption/desorption kinetics, some part of the bound chemicals may desorb within the ventilation volume of the gills, or the chemical may overcome the barrier of unstirred water layer adjacent to the cells bound to TOC as a carrier (so called “facilitated transport”, see section 2.3.2.2). Experimental measurements of uptake efficiencies in the gills in fish suggest that at least up to log K_{ow} 7, facilitated transport by TOC should be negligible (McCarthy and Jimenez, 1985), while model calculations with fast desorption kinetics (which lead to facilitated transport) seem to fit the experimental data for superhydrophobic data better (Erickson and McKim, 1990). Our own simulations indeed show some facilitated transport via TOC for superhydrophobic compounds, see Appendix for details. Yet, prediction of desorption kinetics is quite uncertain, and the resulting differences in rate constants k_1 and k_2 and BCF were small. For this reason, we will assume all chemical bound to TOC as completely non-bioavailable further-on, as is the common approach.

For *Hyalella azteca* experiments, we will calculate with an estimated DOC concentration of about 1 mg DOC/ L_w (personal correspondence with Prof. Schlechtriem, flow-through system, more than 90 % of TOC in water sources is reported to be DOC (Regan et al., 2017)). This leads to a decrease in $f_{unbound}$ with log K_{ow} , as depicted in Figure 3.

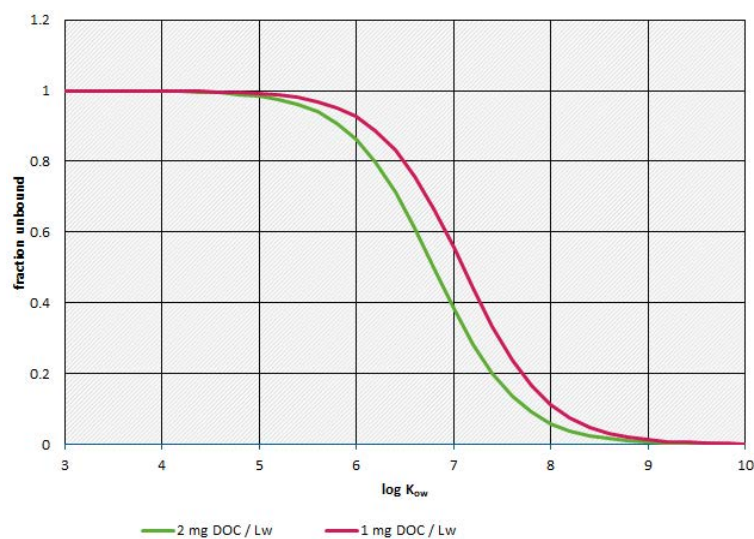
The partition coefficient between the organism and water $K_{org/w}$ describes the equilibrium partitioning between organism and water if only uptake and elimination via the respiratory system is considered, without the influence of total organic matter TOC, or kinetic processes like metabolism or dietary intake/excretion.

The $K_{org/w}$ for hydrophobic chemicals is dominated by their partitioning into the lipid. For the sake of completeness, we also accounted for the partitioning into NLOM and water in the organism. The $K_{org/w}$ is correlated to the K_{ow} according to Equation (5) (Arnot and Gobas, 2004):

$$K_{org/w} = C_{L,org} * K_{ow} + C_{NLOM,org} * 0.035 * K_{ow} + C_{W,org} \quad (5)$$

Where $C_{L,org}$ is the lipid content of the organism, $C_{NLOM,org}$ is the NLOM content, and $C_{W,org}$ the water content of the organism.

Figure 3: Bioavailable fraction $f_{unbound}$



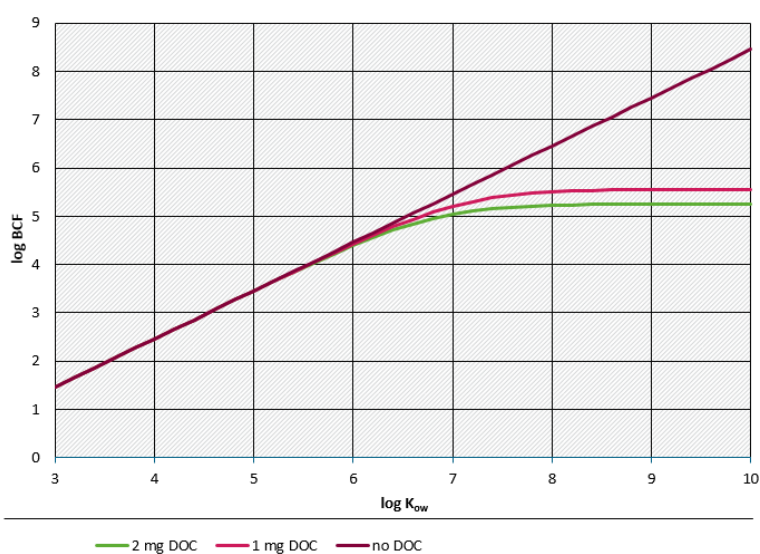
Unbound fraction for 2 different DOC water concentrations depending on log K_{ow}
 Source: own illustration, Helmholtz Centre for Environmental Research GmbH - UFZ

$K_{org/w}$ can also be expressed as the quotient between respiratory uptake rate constant k_1 and respiratory elimination rate constant k_2

$$K_{org/w} = k_1/k_2 \tag{6}$$

Yet, in the presence of TOC, only the bioavailable chemical fraction can be taken up by the gills, decreasing k_1 by the factor $f_{unbound}$. This has direct consequences on the BCF, which does not linearly increase with K_{ow} for high K_{ow} if the DOC is considered, but rather transitions into a plateau, see Figure 4. The final BCF value for extremely hydrophobic compounds then simply represents the partitioning equilibrium between the carbon in water and the lipid in the organism.

Figure 4: BCF if only uptake/elimination over gills is considered



BCF if only uptake/elimination over gills is considered, in absence or presence of DOC (assuming a lipid content of 2%).
 Source: own illustration, Helmholtz Centre for Environmental Research GmbH - UFZ

2.3.2 Diffusion

Many barriers for the uptake (and elimination) of chemicals into the organism are diffusive processes, meaning diffusion is the driving force for the chemical flux. Although in reality it is not realistic to have sharp borders between areas of diffusion and advection (Erickson and McKim, 1990), for simplicity we will strictly separate both processes in the calculations, meaning diffusion is deemed insignificant in areas dominated by water- or bloodflow, and transport in the unstirred water layers or the membrane is solely governed by diffusion.

The diffusive flux is related to the concentration gradient by Fick's first law:

$$J = -D * \frac{dc}{dx} \quad (7)$$

Where J is the diffusive flux (in mass_{chemical}/area/time), D is the diffusion constant, c the chemical concentration and x the position.

Diffusion constants in water are estimated from MW, according to (Avdeef, 2010):

$$D = 10^{-4.13-0.453*\log(MW)} \quad (8)$$

Calculated diffusion constants are listed at the end of the paragraph in Table 7. We assumed equal diffusion coefficients in blood as in water.

2.3.2.1 Unstirred water layer

The concentration of a solute can be assumed uniform if the compartment is well mixed, yet there will always be an unstirred water layer (or aqueous boundary layer ABL) adjacent to the membrane barrier where solute transport is solely governed by diffusive processes. ABL thickness can be lowered by increasing agitation (in case of Hyalella for example an increased beating of the pleopods, where the gills reside, and an increased swimming velocity should decrease ABL thickness) or flow, but it can never be completely eliminated. Depending on the solvent permeability in the membrane, ABL permeability might be a limiting process, which is even more likely for superhydrophobic compounds, because they are expected to have high membrane permeabilities. The rate at which the solute moves across the ABL depends on the diffusion coefficient (and therefore on molecule size), the thickness of the ABL, and the concentration difference. The rate constant for diffusion across the ABL k_{ABL} ($L_w/d/kg_{org}$) can be expressed as follows:

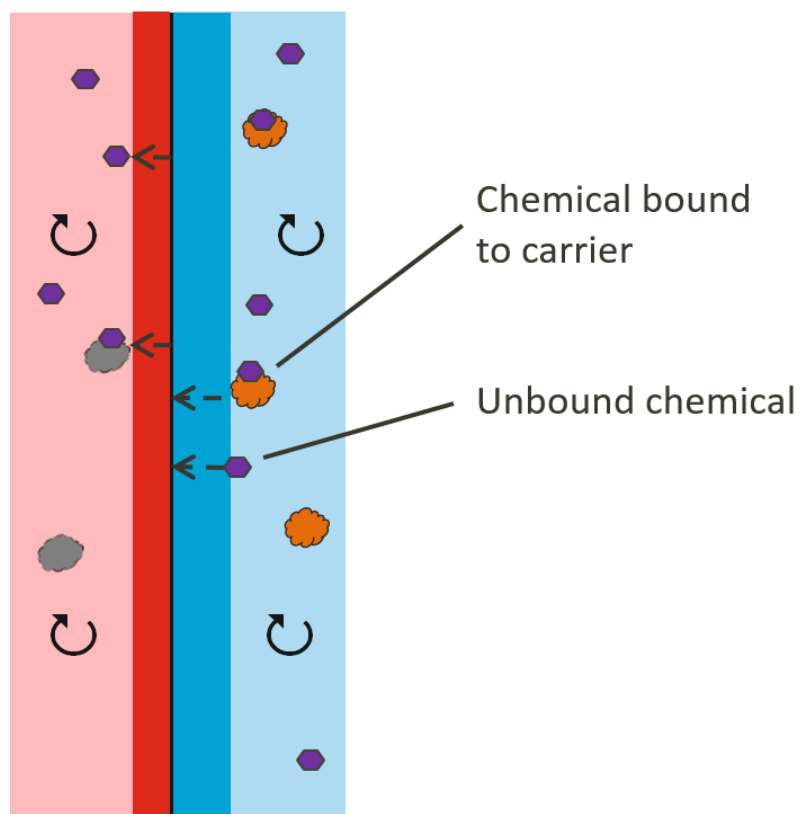
$$k_{ABL} = \frac{D * A}{d_{ABL}} / M_{org} \quad (9)$$

Where D is the aqueous diffusion coefficient, A is the surface area, d_{ABL} is the ABL thickness, and M_{org} is the wet weight of the organism.

2.3.2.2 Facilitated transport

For strongly hydrophobic compounds, it is not the membrane itself that represents the highest resistance for permeation across epithelial cells, but the layers of unstirred water adjacent to the membrane, that can only be traversed by passive diffusion. The low passive diffusion across this layer by the chemical can be increased by so called “facilitated transport”, see Figure 5. The chemical binds to the carrier, and is transported across the ABL by diffusion of the carrier. The resulting permeability depends on the partitioning of the chemical between water and carrier, and on the diffusion constant of the carrier. The sorption and desorption kinetics between the solute and the carrier might also be rate limiting, in which case the facilitation factor also depends on the ABL thickness.

Figure 5: Facilitated transport



Facilitated transport depicted for blood and water. The compound may traverse the ABL on its own or bound to a carrier.
Source: own illustration, Helmholtz Centre for Environmental Research GmbH - UFZ

In the extreme case of extremely slow sorption kinetics, the fraction bound is not bioavailable. Although the solute might traverse the ABL bound to a carrier, there will be no facilitated transport if it takes considerably longer for the compound to desorb from the carrier than to diffuse on its own. We expect such slow sorption kinetics for TOC, see section 2.3.1.

If there is no limitation by de-/sorption kinetics, the facilitation factor FAC can be expressed as follows (Larisch and Goss, 2018b):

$$FAC = \frac{P_{passive\ diffusion}^{ABL} + P_{carrier\ bound}^{ABL}}{P_{passive\ diffusion}^{ABL}} \quad (10)$$

Where $P_{passive\ diffusion}^{ABL}$ is the permeability across the ABL without facilitated transport, and $P_{carrier\ bound}^{ABL}$ the permeability across the ABL bound to the carrier.

$$P_{carrier\ bound}^{ABL} = \frac{D_{carrier} * K_{carrier/water} * c_{carrier}}{d_{ABL}} \quad (11)$$

Where $D_{carrier}$ is the diffusion coefficient of the carrier in water, $K_{carrier/water}$ is the carrier/water partition coefficient, $c_{carrier}$ is the carrier concentration and d_{ABL} is the thickness of the ABL.

In case of finite de-/sorption rates, it is necessary to calculate the de-/sorption processes in parallel to the diffusion process. It is needed to split the ABL in different layers, as de-/sorption processes take place during the whole diffusion process. A molecule only carried the last little stretch of the way will not contribute the same way to the facilitation factor as a molecule picked up from the start. For a blood ABL of 286 nm, calculating with 10 different layers resulted in a

facilitation factor 10 times lower than when only one layer had been used for calculation, see Appendix A.2. The resulting facilitation factors are listed in Table 7 and 8.

The ABL in the gut is reported to be 50 - 2 000 μm thick in humans (Kelly et al., 2004). For the calculations in fish and *Hyalella azteca*, we will assume an ABL thickness of 137 μm , as this size was used determining an empirical correlation to assess the facilitated transport of compounds carried by bile acids in the gut (Westergaard and Dietschy, 1976). Resulting facilitation factors are listed in Table 7 and 8, and details on their prediction can be found in Appendix A.3 .

2.3.3 Cell permeation

For the permeation of the cell layer in the gills or the gut, we consider two parallel diffusion paths: The chemical might either traverse the cell membrane, diffuse through the cytosol, and then traverse the opposite cell membrane, or it might diffuse directly within the membrane without entering the cytosol, the so called lateral transport (Bittermann and Goss, 2017). For very hydrophilic chemicals, it is not energetically favorable to reside in the membrane, the dominating transport path will thus lead through the cytosol. Yet, the membrane itself should not pose a barrier to superhydrophobic compounds, for which lateral transport will dominate.

$$P_{cell}^{total} = P_{cyt}^{tot} + P_{lateral} = \frac{1}{2 * R_{mem} + R_{cyt}} + \frac{1}{R_{lateral}} \quad (12)$$

Where P_{cell}^{total} is the total cell permeability, P_{cyt}^{tot} is the total permeability across the cytosolic route, R_{mem} is the resistance for membrane permeation, R_{cyt} is the resistance for the diffusion across the cytosol, and $R_{lateral}$ is the resistance across the lateral route. Details can be found in Appendix A.4.

The cell permeation rate constant k_{cell} (in $L_w/d/kg_{org}$) can be expressed as follows:

$$k_{cell} = P_{cell}^{total} * A/M_{org} \quad (13)$$

Where A is the surface area of the respective organ, and M_{org} the mass of the organism.

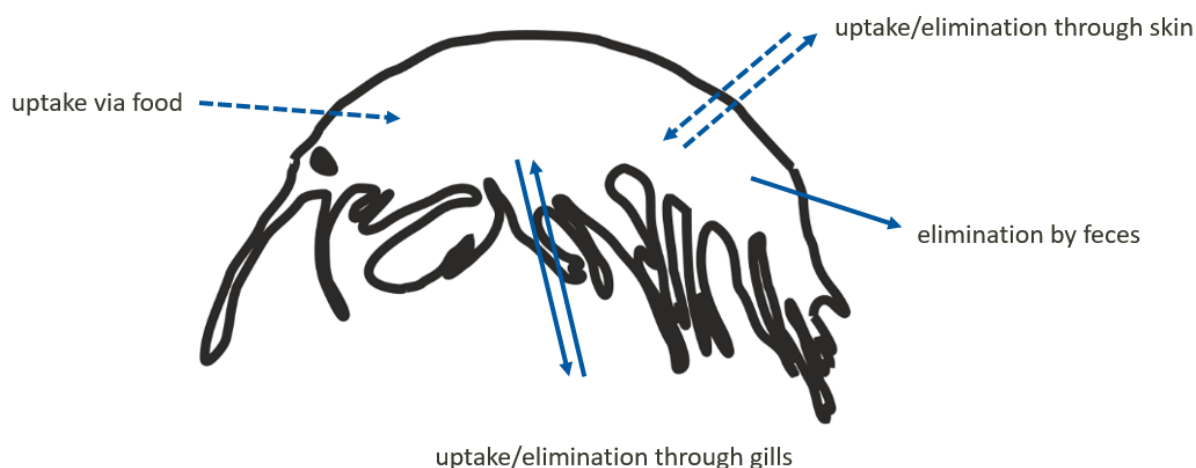
2.3.4 Bloodflow

In contrast to fish, crustaceans possess an open circulatory system, with nutrients, oxygen, hormones, and cells distributed in the hemolymph (Fredrick and Ravichandran, 2012). The classical concept of bloodflow through blood vessels like in fish is therefore not applicable, the blood flows freely through cavities. For *Hyalella azteca*, we therefore are not able to depict the influence of bloodflow on the overall kinetics. But we hope for the resulting error to be small, because at least in fish, bloodflow should be rather limiting for hydrophilic chemicals, but not for superhydrophobic compounds, due to the increased binding to albumin with increasing K_{ow} , and the resulting facilitated transport.

2.4 Identification of relevant uptake/elimination paths in *Hyalella azteca*

In this section, we take a closer look at the various possible uptake and elimination paths and their relevance. Uptake and elimination via the gills, and the elimination by feces were identified as the most important ones. Uptake via skin and food were deemed irrelevant. For simplicity, it was assumed that the blood is in equilibrium with the organism.

Figure 6: Considered uptake and elimination paths



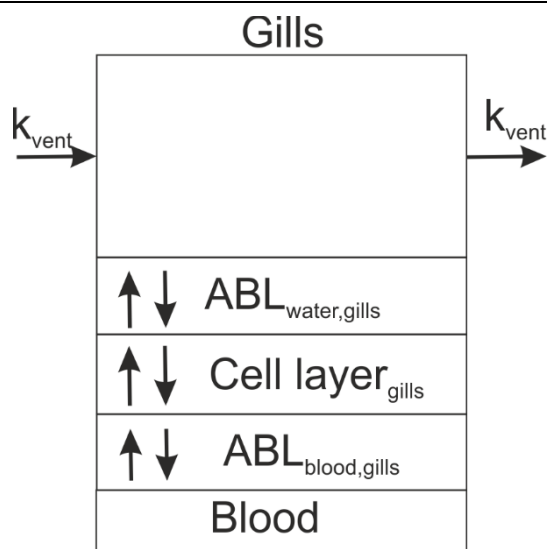
Scheme of considered uptake and elimination paths in *H. azteca*.

Source: own illustration, Helmholtz Centre for Environmental Research GmbH - UFZ

2.4.1 Uptake/elimination via gills

The modeled uptake/elimination via the gills is comprised of several resistances in series: ventilation (k_{vent}), diffusion through the ABL in water adjacent to the gills, permeation through the cell monolayer in the gills, and diffusion through the ABL in blood, as depicted in Figure 7.

Figure 7: Uptake and elimination via gills

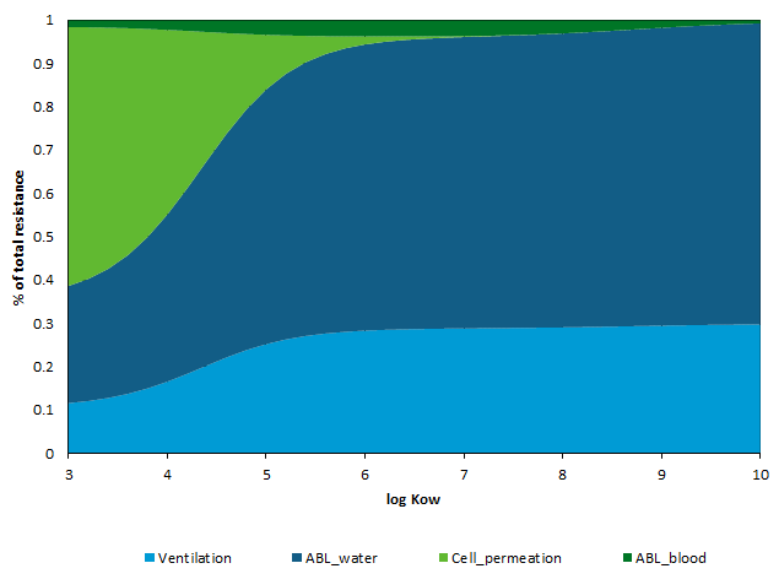


Scheme of the uptake and elimination via gills.

Source: own illustration, Helmholtz Centre for Environmental Research GmbH – UFZ

The ABL in water was assumed to be 5 μm (SUTCLIFFE, 1984). Cell layer thickness was assumed to be 6.4 μm as in rainbow trout (Hughes, 1970) for the calculations. Although this value might differ in *Hyalomma azteca*, this should not be relevant for the superhydrophobic chemicals, because cell permeation only seems to pose a significant resistance for low K_{ow} , see Figure 8. Note that no facilitated transport by TOC as carrier was assumed in the ABL in water.

Figure 8: Importance of single resistances in gills



Modeled importance of single resistances in gills in *Hyalella azteca*. Bloodflow is not considered, but should have significant impact for low K_{ow} values.

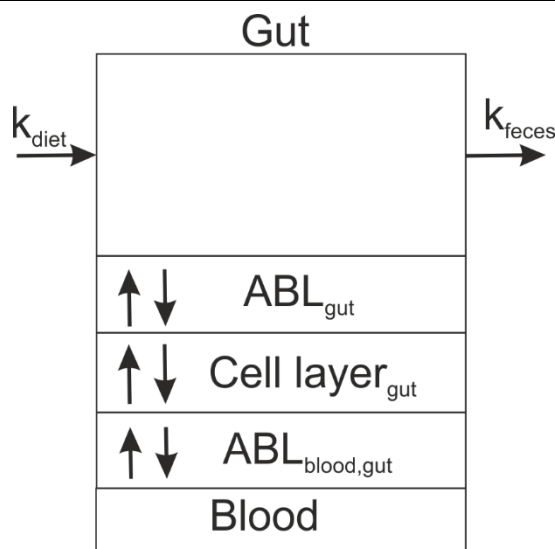
Source: own illustration, Helmholtz Centre for Environmental Research GmbH – UFZ

According to the model, the diffusion through the ABL in water is the main resistance in the gills for superhydrophobic compounds.

2.4.2 Uptake/elimination via gut

The modeled uptake/elimination via the gut is comprised of several resistances in series: diet/feces (k_{diet}/k_{feces}), diffusion through the ABL in the gut, permeation through the cell layer in the gut, and diffusion through the ABL in blood, as depicted in Figure 9. In the case of BCF measurements, k_{diet} can be set to 0, because feeding was done with uncontaminated food.

Figure 9: Uptake and elimination via gut



Scheme of the uptake and elimination via gut.

Source: own illustration, Helmholtz Centre for Environmental Research GmbH - UFZ

The ABL in the gut was assumed to be 137 μm (see section 2.3.2.2). Gut cell layer thickness was assumed to be 11 μm as in 28 days old rainbow trout (Minghetti et al., 2017) for the calculations. Although this value might differ in *Hyaella azteca*, this should not be relevant, because cell permeation seems to pose no significant resistance, see Figure 10.

Feeding was done ad libitum, with fish feed embedded in an agar matrix (Kampfraath et al., 2012), consisting of 23 ml water, 1500 mg ground and 500 mg agar-agar (Schlechtriem et al., 2021). We calculated the final composition of the DECOTAB as $0.924 \text{ kg}_{\text{water}}/\text{kg}_{\text{diet}}$, $0.07 \text{ kg}_{\text{NLOM}}/\text{kg}_{\text{diet}}$, and $0.007 \text{ kg}_{\text{lipid}}/\text{kg}_{\text{diet}}$. Assuming a similar feeding rate G_d as for *A. aquaticus* with $3 \text{ mg}_{\text{diet,dry}}/\text{d}/(5 \text{ animals})$ (Kampfraath et al., 2012), with a wet weight of 12 mg for *A. aquaticus* of 8 mm length (Fitzpatrick, 1968), this leads to a feeding rate of $0.05 \text{ mg}_{\text{diet,dry}}/\text{d}/\text{kg}_{\text{org}}$, or $0.65 \text{ mg}_{\text{diet,wet}}/\text{d}/\text{kg}_{\text{org}}$. The feeding rate calculated after (Arnot and Gobas, 2004) is quite similar, with resulting $0.59 \text{ mg}_{\text{diet,wet}}/\text{d}/\text{kg}_{\text{org}}$:

$$G_d = 0.022 * BW^{0.85} * \exp(0.06 * T) \quad (14)$$

Where BW is the body weight and T the temperature, here 23°C.

G_d of $0.65 \text{ mg}_{\text{diet,wet}}/\text{d}/\text{kg}_{\text{org}}$ was used for the calculations.

Fecal egestion rate ($\text{kg}_{\text{feces}}/\text{kg}_{\text{org}}/\text{d}$) was calculated from the feeding rate, assimilation efficiencies and dietary composition as described in (Arnot and Gobas, 2004):

$$G_F = \{(1 - \varepsilon_L) * v_{LD} + (1 - \varepsilon_N) * v_{ND} + (1 - \varepsilon_W) * v_{WD}\} * G_d \quad (15)$$

Where ε_L , ε_N , and ε_W are the dietary assimilation efficiencies of lipid, NLOM, and water, respectively, as listed in Table 1, and v_{LD} , v_{ND} and v_{WD} the lipid, NLOM and water contents of the diet, respectively.

The feces/water partition coefficient can be expressed as:

$$K_{F/W} = K_{ow} * v_{LF} + K_{ow} * v_{NF} + v_{WF} \quad (16)$$

Where v_{LF} , v_{NF} and v_{WF} are the lipid, NLOM and water contents of the feces, respectively, which are calculated as follows:

$$v_{LF} = (1 - \varepsilon_L) * v_{LD} / \{(1 - \varepsilon_L) * v_{LD} + (1 - \varepsilon_N) * v_{ND} + (1 - \varepsilon_W) * v_{WD}\} \quad (17)$$

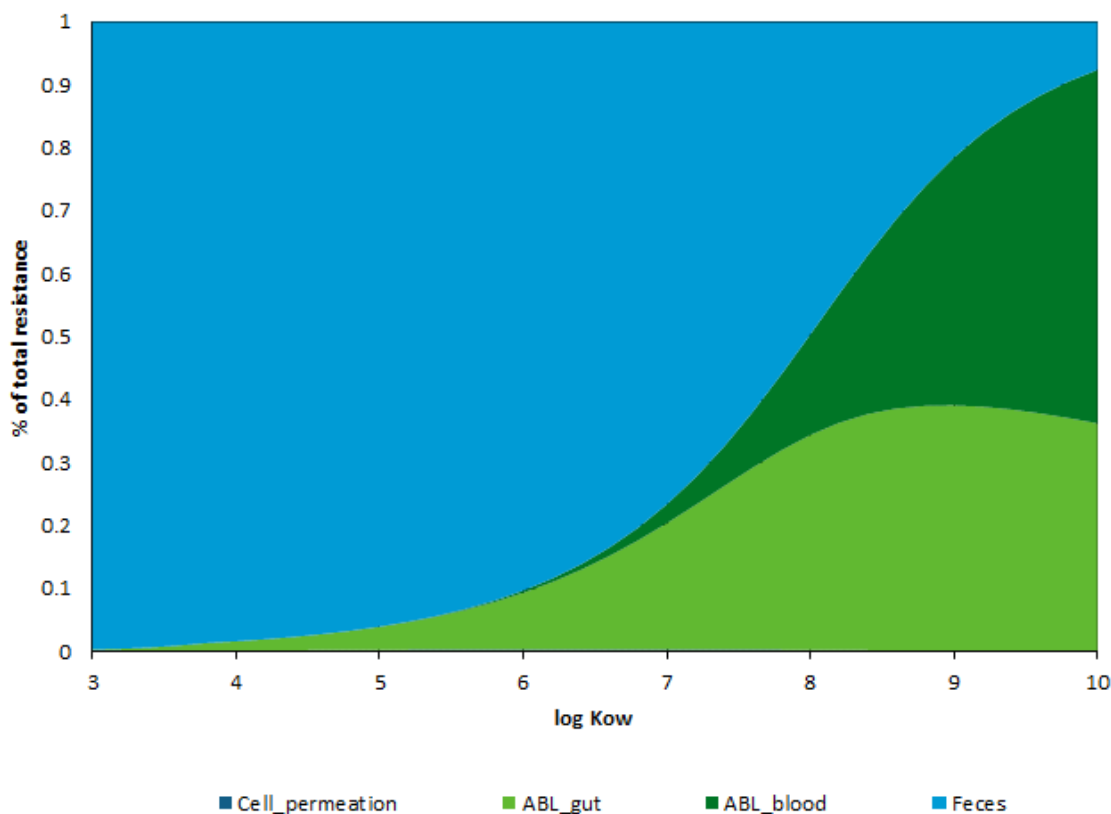
$$v_{NF} = (1 - \varepsilon_N) * v_{ND} / \{(1 - \varepsilon_L) * v_{LD} + (1 - \varepsilon_N) * v_{ND} + (1 - \varepsilon_W) * v_{WD}\} \quad (18)$$

$$v_{WF} = (1 - \varepsilon_W) * v_{WD} / \{(1 - \varepsilon_L) * v_{LD} + (1 - \varepsilon_N) * v_{ND} + (1 - \varepsilon_W) * v_{WD}\} \quad (19)$$

k_{feces} (in $\text{L}_w/\text{kg}_{\text{org}}/\text{d}$) can then be expressed by:

$$k_{\text{feces}} = K_{F/W} * G_F \quad (20)$$

Figure 10: Importance of single resistances in gut



Modeled importance of single resistances in gut in *Hyalella azteca*. Bloodflow is not considered.
 Source: own illustration, Helmholtz Centre for Environmental Research GmbH - UFZ

2.4.3 Uptake/elimination via skin (deemed irrelevant)

Hyalella azteca is much smaller than fish, therefore a higher surface area to volume ratio is expected. Skin permeation might thus be more relevant than in fish. We estimated skin surface area to be only about a factor of 3 higher than gill area. Taking into account thicker cell layers instead of the cell monolayer at the gills, the chitin shell, and a thicker ABL than in the gills, skin permeation should be insignificant as compared to the uptake through the gills.

2.4.4 Elimination via metabolism

Metabolism can be an important elimination path, but was not in the general scope of this work. We have no data on metabolic rates in *Hyalella azteca*, which might differ between fish and *Hyalella azteca*. Nevertheless, we will use predicted metabolism rates in fish (Brown et al., 2012)(EAS-E Suite) to test our predicted k_2 values against experimental results, to assess whether metabolism might have been a relevant process.

2.5 Calculation of k_1 and k_2

2.5.1 Resulting rate constants

In the model, we assume instant equilibrium between the blood and the organism. There is only uptake via gills, as the food is uncontaminated ($k_{diet}=0$). Elimination via gills $k_{2,gills}$ and via the gut $k_{E,gut}$ are parallel processes, the whole-body rate constants can therefore be added:

$$k_2 = k_{2,gills} + k_{E,gut} \quad (21)$$

The single resistances in the gills (and gut) are connected in series. In a steady state situation, intermediate concentrations are constant, and the systems of equations in Table 3 and 4 have to be fulfilled.

Table 3: System of equations gills

| Equation | C_{vent} | $C_{ABL,gill}$ | $C_{ABL,blood}$ | C_{org} | C_w | |
|----------|--|---|---|-----------------------------|---------------------------|----------|
| I | $-f_{unbound} * k_{vent}$ $- f_{unbound} * k_{ABL,w}$ | $+ f_{unbound} * k_{ABL,w}$ | 0 | 0 | $-f_{unbound} * k_{vent}$ | 0 |
| II | $+ f_{unbound} * k_{ABL,w}$ | $- f_{unbound} * k_{ABL,w}$ $- f_{unbound} * k_{cell,gills}$ | $+ k_{cell,gills}$ | 0 | 0 | 0 |
| III | 0 | $+ f_{unbound} * k_{cell,gills}$ | $- k_{cell,gills}$ $- k_{ABL,blood}$ | $+ k_{ABL,blood}/K_{org/w}$ | 0 | 0 |
| IV | 0 | 0 | $+ k_{ABL,blood}$ | $- k_{ABL,blood}/K_{org/w}$ | 0 | $- \Phi$ |

$f_{unbound}$ unbound fraction, k_{vent} ventilation rate constant, $k_{ABL,w}$ rate constant for diffusion in aqueous ABL adjacent to gills, $k_{cell,gills}$ rate constant for diffusion through cell monolayer, $k_{ABL,blood}$ rate constant for diffusion through ABL in blood, Φ the resulting flux, C_{vent} is the concentration in the ventilation volume, $C_{ABL,gills}$ is the concentration in the aqueous ABL adjacent to the gill membrane, $C_{ABL,blood}$ is the concentration in the blood ABL adjacent to the gill cells, C_{org} is the concentration in the organism, at equilibrium with the blood, C_w is the concentration in water. Equation I corresponds to the change in C_{vent} , which is zero at steady state: $(-f_{unbound} * k_{vent} - f_{unbound} * k_{ABL,w}) * C_{vent} + f_{unbound} * k_{ABL,w} * C_{ABL,gills} - f_{unbound} * k_{vent} * C_w = 0$, and so on.

Table 4: System of equations gut

| Equation | C_{gut} | $C_{ABL,gut}$ | $C_{ABL,blood}$ | C_{org} | |
|----------|-----------------------------|--------------------------------|----------------------------------|-----------------------------|--------------|
| I | $- k_{feces} - k_{ABL,gut}$ | $+ k_{ABL,gut}$ | 0 | 0 | $- k_{diet}$ |
| II | $+ k_{ABL,gut}$ | $- k_{ABL,gut} - k_{cell,gut}$ | $+ k_{cell,gut}$ | 0 | 0 |
| III | 0 | $+ k_{cell,gut}$ | $- k_{cell,gut} - k_{ABL,blood}$ | $+ k_{ABL,blood}/K_{org/w}$ | 0 |
| IV | 0 | 0 | $+ k_{ABL,blood}$ | $- k_{ABL,blood}/K_{org/w}$ | $- \Phi$ |

k_{feces} rate constant for feces, $k_{ABL,gut}$ rate constant for diffusion in aqueous ABL in gut, $k_{cell,gut}$ rate constant for diffusion through cell monolayer, $k_{ABL,blood}$ rate constant for diffusion through ABL in blood, Φ the resulting flux, C_{gut} is the concentration in the gut volume, $C_{ABL,gut}$ is the concentration in the aqueous ABL adjacent to the gut cells, $C_{ABL,blood}$ is the concentration in the blood ABL adjacent to the gut cells, C_{org} is the concentration in the organism, at equilibrium with the blood.

Solving these systems of equations leads to the following uptake and elimination rates:

$$k_{1,gills} = f_{unbound} * (k_{ABL,blood} * k_{cell,gills} * k_{ABL,gills} * k_{vent}) / (k_{ABL,blood} * k_{cell,gills} * k_{ABL,gills} + k_{cell,gills} * k_{ABL,gills} * k_{vent} + k_{ABL,blood} * k_{ABL,gills} * k_{vent} + k_{ABL,blood} * k_{cell,gills} * k_{vent}) \quad (22)$$

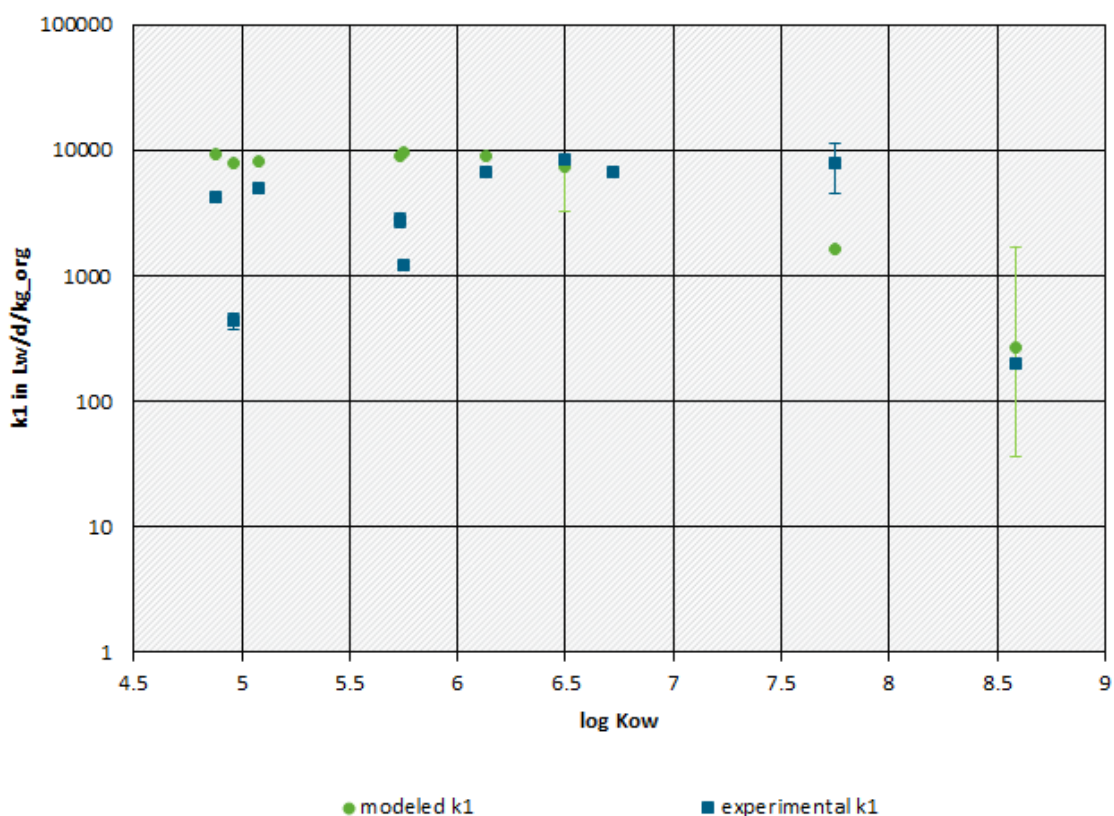
$$k_{2,gills} = (k_{ABL,blood} * k_{cell,gills} * k_{ABL,gills} * k_{vent}) / (k_{ABL,blood} * k_{cell,gills} * k_{ABL,gills} + k_{cell,gills} * k_{ABL,gills} * k_{vent} + k_{ABL,blood} * k_{ABL,gills} * k_{vent} + k_{ABL,blood} * k_{cell,gills} * k_{vent}) / K_{org/w} \quad (23)$$

$$k_{E,gut} = \frac{(k_{ABL,blood} * k_{cell,gut} * k_{ABL,gut} * k_{feces}) / (k_{ABL,blood} * k_{cell,gut} * k_{ABL,gut} + k_{cell,gut} * k_{ABL,gut} * k_{feces} + k_{ABL,blood} * k_{ABL,gut} * k_{feces} + k_{ABL,blood} * k_{cell,gut} * k_{feces}) / K_{org}}{w} \quad (24)$$

2.5.2 Comparison of modeled to experimental k1

To allow for a direct comparison of modeled k1 to experimental k1 measured by (Schlechtriem et al., 2019) and (Schlechtriem et al., 2021), calculations were done with a 2% lipid content of the organism and 1 mg /L_w DOC (measured DOC concentrations, personal correspondence with the author). For UV-329 and UV-234, log K_{ow} predictions differ strongly between single prediction methods (see Section 2.2.2). Using the mean of the predicted log K_{ow} of UV-234 (8.6±0.9) and of UV-329 (6.5±0.9), the resulting k1 are 2.7*10² L_w/d/kg_{org} and 7.4*10³ L_w/d/kg_{org} respectively, which is quite similar to the experimental values of 2.0*10² and 8.3*10³ L_w/d/kg_{org} (Schlechtriem et al., 2021). Yet, the range of possible results is extremely large due to the K_{ow} uncertainty, with 4.2*10¹ -2.0*10³ and 4.1*10³ -1.0*10⁴ L_w/d/kg_{org} respectively (limits were calculated using the mean log K_{ow} values plus/minus the standard deviation). The resulting k1 values are also listed in Table 9 and 11, alongside the values predicted for several hydrophobic compounds measured in (Schlechtriem et al., 2019), and depicted in Figure 11.

Figure 11: Modeled and experimental k1



Modeled and experimental k1 in *Hyalella azteca*. The k1 were modeled for a 3 mg organism with 2% lipid content and 1 mg DOC/L_w. Blue error bars represent the standard error of the experiment, green error bars the uncertainty in modeled k1 due to uncertain prediction of log K_{ow}.

Source: own illustration, Helmholtz Centre for Environmental Research GmbH - UFZ

The three largest outliers, hexachlorobenzene, ortho-terphenyl, and chlorpyrifos (log K_{ow} 5.73, 5.75, and 4.96, respectively), might be due to experimental problems. For these uptake curves,

time resolution seems insufficient, or the uptake curve shows broad scatter. PCB153 ($\log K_{ow}$ 7.62) did not reach steady state during the uptake period, which might explain the large experimental error.

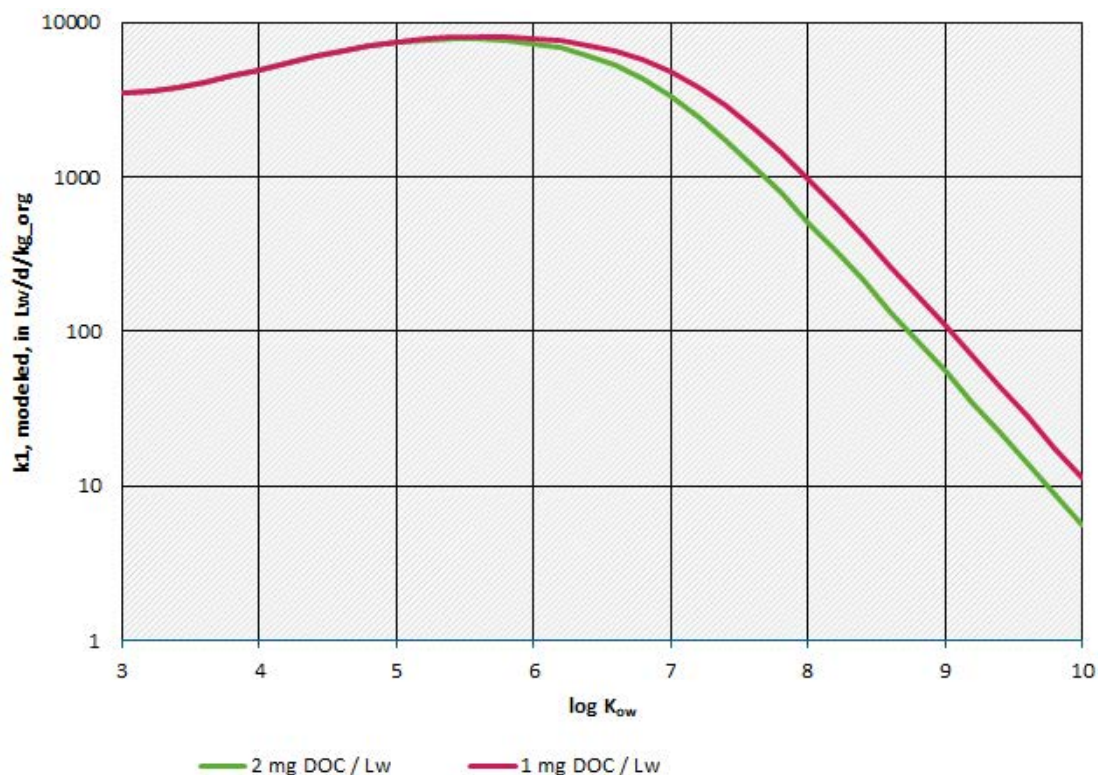
The k_1 values of chemicals with a $\log K_{ow}$ below 6.5 seem to be consistently overestimated. The reason might be that in that range, bloodflow could be a limiting factor. As it was not incorporated in the model due to lack of physiological data, this would lead to an overestimation of k_1 .

Overall, the modeled k_1 for superhydrophobic compounds seem to be mechanistically explainable. The decrease in k_1 for high $\log K_{ow}$ is a consequence of the chemical's binding to TOC, which results in a lowered bioavailable unbound fraction in water.

2.5.3 k_1 depending on K_{ow}

To model the typical course of k_1 with $\log K_{ow}$, the input parameters had to be expressed in dependence of K_{ow} . Although some correlations are established, such as the binding to albumin (Endo and Goss, 2011), or the membrane permeability (Walter and Gutknecht, 1986), the predicted micelle facilitation factor, while correlating with $\log K_{ow}$, scatters widely (see Figure 20). Also, the curves had to be modeled for a specific molecular weight (400 g/mol in the example curves below), which will affect the molecule's diffusion constant and de-/sorption kinetics to albumin. Figure 12 must therefore be understood to only show a general trend, but individual input parameters should be used for the chemical of interest to derive more exact predictions.

Figure 12: Modeled k_1 depending on K_{ow}



Modeled k_1 in *Hyalella azteca* depending on $\log K_{ow}$. The k_1 were modeled for a 3 mg organism with 2% lipid content, in the presence of 1 mg / L_w DOC or 2 mg / L_w DOC. The modeling was done for a compound with MW of 400 g/mol. Source: own illustration, Helmholtz Centre for Environmental Research GmbH - UFZ

2.5.4 Limits of applicability

The model overestimates k_1 for chemicals with $\log K_{ow}$ below 6.5, likely because bloodflow is not incorporated in the model. For $\log K_{ow}$ above 6.5, the model seems to mostly match experimental data (for the few experimental data available), yet both experimental and modeled data are quite uncertain in that range. A measurement of the actual unbound fraction in water should improve predictions, because predicting the binding to TOC is based on an extrapolation far beyond the initial training of the empirical QSAR (Burkhard, 2000). The lack of experimental $\log K_{ow}$ (or their unreliability) and the strong deviations between different $\log K_{ow}$ prediction methods will propagate uncertainty to predicted k_1 . Also, for superhydrophobic chemicals, it is not clear whether some of the fraction bound to TOC is still bioavailable, in which case the model would underestimate k_1 for these chemicals. Note that the model in its current form is only valid for neutral compounds.

3 Workpackage 2: Suitability of the Hyalella BCF test for superhydrophobic substances

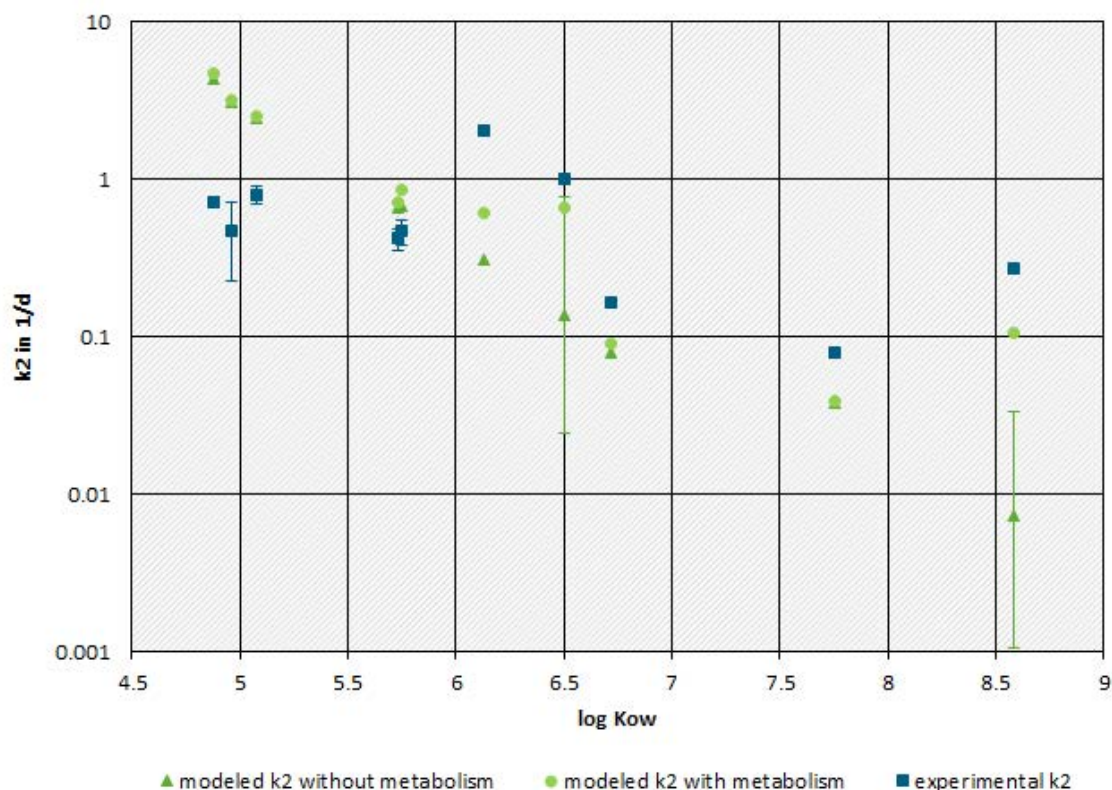
3.1 Modeled k2 to estimate time till steady state

For both UV-234 and UV-329, the modeled k2 values of $7.28 \cdot 10^{-3}$ 1/d and $1.36 \cdot 10^{-1}$ 1/d, respectively, are well below the experimentally measured k2 of $2.7 \cdot 10^{-1}$ 1/d and $9.9 \cdot 10^{-1}$ 1/d, respectively. Metabolism seems to be the most likely explanation. In that case, Equation (21) is supplemented by metabolism:

$$k_2 = k_{2,gills} + k_{E,gut} + k_{metabolism} \quad (25)$$

Using predicted fish biotransformation half-lives (Brown *et al.*, 2012; EAS-E Suite) of 168.16 h and 32.33 h, for these compounds respectively, the resulting k2 with $1.1 \cdot 10^{-1}$ 1/d and $6.5 \cdot 10^{-1}$ 1/d fit much better to the experimental values. Including metabolism in the calculation also improves the prediction for other chemicals from (Schlechtriem *et al.*, 2019), see Figure 13.

Figure 13: Modeled and experimental k2



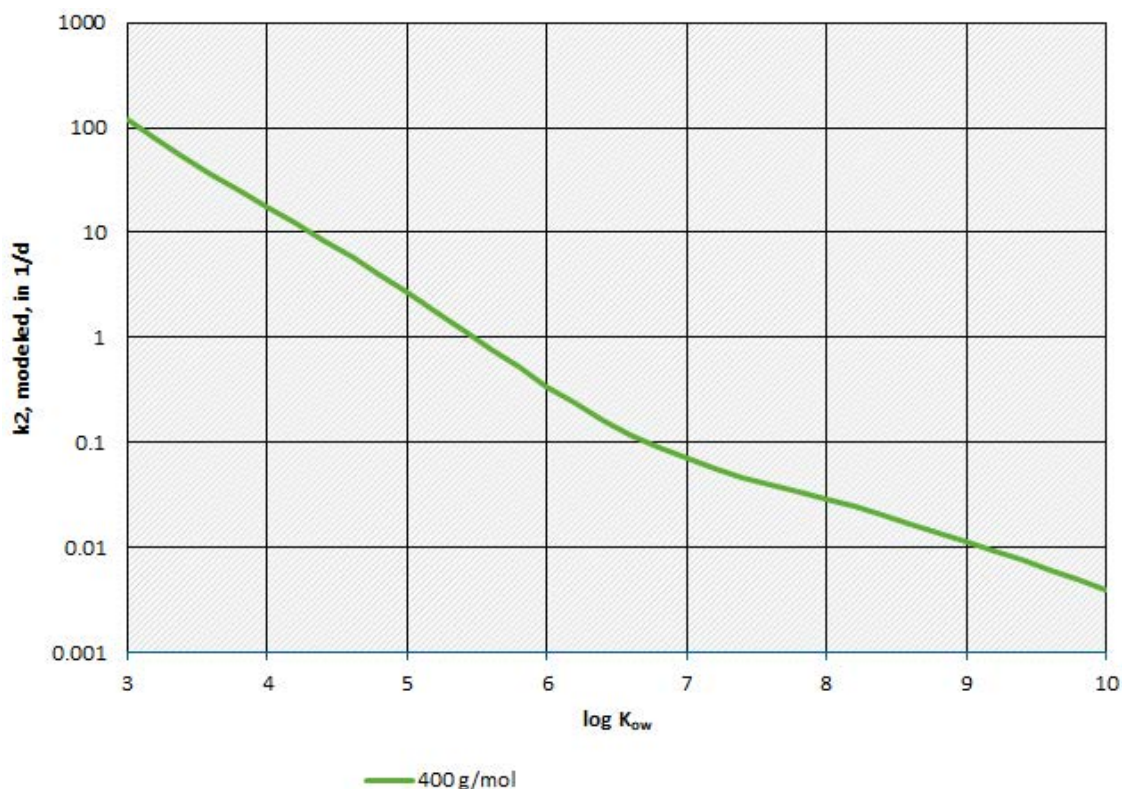
Modeled and experimental k2 in *Hyalella azteca*. The k2 were modeled for a 3 mg organism with 2% lipid content. Blue error bars represent the standard error of the experiment, green error bars the uncertainty in modelled k2 due to uncertain prediction of log K_{ow}.

Source: own illustration, Helmholtz Centre for Environmental Research GmbH - UFZ

Like for k1, most k2 are overestimated for log K_{ow} < 6.5, which again could be a consequence of neglecting bloodflow in the modeling. Figure 14 shows the typical course of modeled k2 in dependence of log K_{ow} in the absence of metabolism. Like for k1, Figure 14 must be understood to only show a general trend, individual input parameters should be used for the chemical of

interest to derive more exact predictions. According to the model, for superhydrophobic substances, the ABL in blood and in the gut are the main resistances for k_F . Both resistances are most unreliable in their prediction, as assumptions to ABL sizes and facilitation factors were made that seem to work well for fish, but have not been tested for *Hyalella azteca*. Unfortunately, the sparsity of data points in the high hydrophobicity range and the influence of metabolism make it impossible to systematically check the predicted k_2 values against experimental values. Their prediction is therefore less reliable.

Figure 14: Modeled k_2 depending on K_{ow}



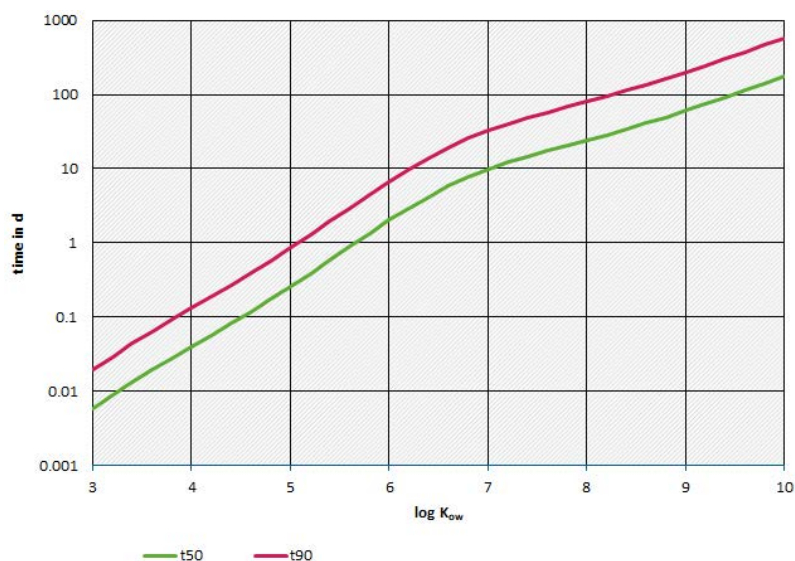
Modeled k_2 in *Hyalella azteca* depending on $\log K_{ow}$. The k_2 were modeled for a 3 mg organism with 2% lipid content. The modeling was done for a compound with MW of 400 g/mol, assuming no metabolism. Source: own illustration, Helmholtz Centre for Environmental Research GmbH - UFZ

Assuming first order kinetics, the time to reach 50% of steady state t_{50} can be calculated as follows:

$$t_{50} = \frac{-\ln(1 - 0.50)}{k_2} \quad (26)$$

According to these calculations, for superhydrophobic compounds, it may even take more than 100 days to reach 50% of steady state (in the absence of metabolism), which is not practical in a standard test. Note: Due to neglecting the influence of bloodflow, overestimated k_2 for low K_{ow} values might lead to underestimated t_{50} in that low range.

Figure 15: Estimated t50 of depuration phase



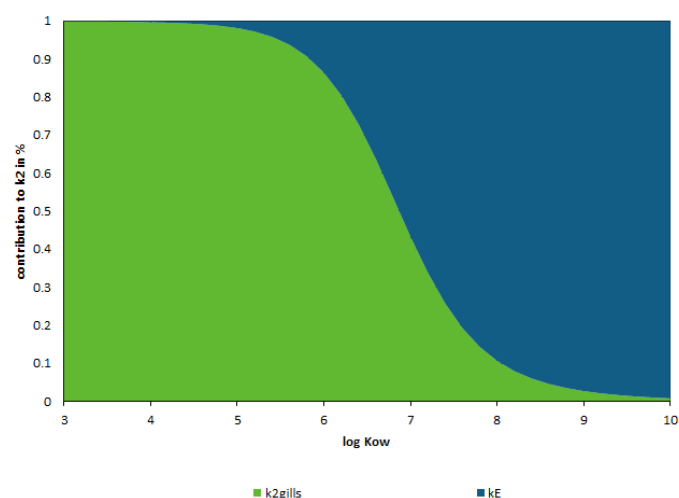
Modeled time to reach steady state (50% or 90% respectively) in *Hyalella azteca* depending on log K_{ow}. The times were calculated for a 3 mg organism with 2% lipid content. The modeling was done for a compound with MW of 400 g/mol, assuming no metabolism.

Source: own illustration, Helmholtz Centre for Environmental Research GmbH - UFZ

3.2 BCF

If there is no metabolism and no diet, the log BCF is expected to run into a plateau in the presence of TOC for high log K_{ow}, see Figure 4. Yet, if uncontaminated diet is provided, this opens up an additional elimination path that gains importance with increasing log K_{ow}, see Figure 16.

Figure 16: Contributions of k_{2,gills} and k_E to k₂



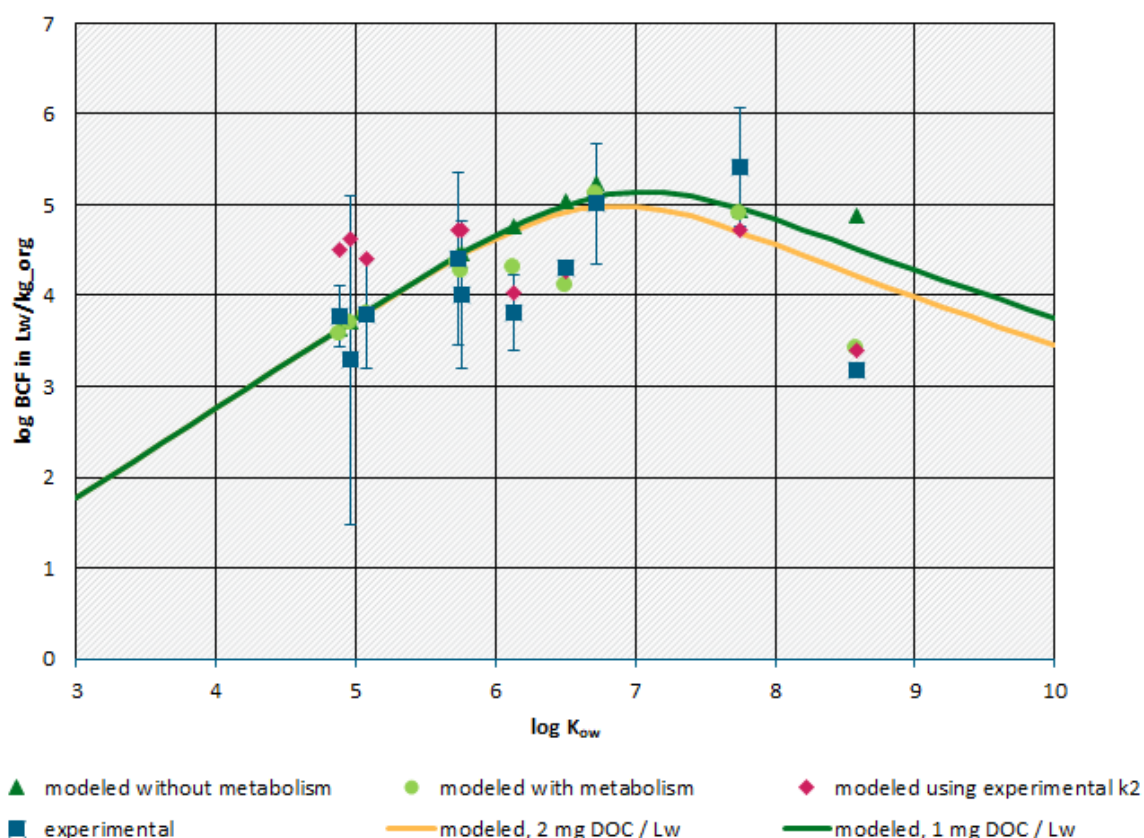
Modeled contributions of k_{2,gills} and k_E (gut) to k₂. The contributions were calculated for a 3 mg organism with 2% lipid content. The modeling was done for a compound with MW of 400 g/mol, assuming no metabolism.

Source: own illustration, Helmholtz Centre for Environmental Research GmbH - UFZ

In that case, the BCF will decrease with higher log K_{ow}. This leads to the lower experimental log BCF for UV-234 than for UV-329 (experimental log BCF 3.2 and 4.3 respectively), which is

counter-intuitive, as UV-234 has a much larger $\log K_{ow}$. This trend is also evident for our modeled BCF, see Figure 17. Lines in Figure 17 show the typical course of modeled BCF in dependence of $\log K_{ow}$, in the absence of metabolism. Curves must be understood to only show a general trend, but individual input parameters should be used for the chemical of interest to derive more exact predictions. Nevertheless, modeled values seem to fit the experimental values, the strongest outliers being those compounds for which significant metabolic activity is expected.

Figure 17: Log BCF for (super)hydrophobic chemicals



Experimental and modeled BCF for (super)hydrophobic chemicals. The values were calculated for a 3 mg organism with 5% lipid content. Modeling was done without metabolism (dark green dots), with metabolism (light green dots), or calculating the BCF dividing the modelled k_1 by the experimental k_2 (rose dots). Experimental kinetic BCF (for 5% lipid content) is depicted in blue, with the uncertainty stated in (Schlechtriem *et al.*, 2019). Modeled lines represent the $\log BCF$ depending on $\log K_{ow}$, in the presence of 1 mg DOC/L_w and 2 mg DOC/L_w, respectively, for chemicals with MW of 400 g/mol and in the absence of metabolism.

Source: own illustration, Helmholtz Centre for Environmental Research GmbH - UFZ

3.3 Comparability between BCF studies with fish and Hyalella azteca

Modeling the BCF using physiological data for *Hyalella azteca* and rainbow trout, respectively, the resulting curves are quite similar, see Figure 18. This agrees with (Schlechtriem *et al.*, 2019) who observed a tendency for BCF to be higher in *Hyalella azteca* than in fish, but still observed a clear correlation.

Although experimental BCF in *Hyalella azteca* are smaller for UV-234 than UV-329, the same is not observed in rainbow trout (REACH registration dossier for UV-329).

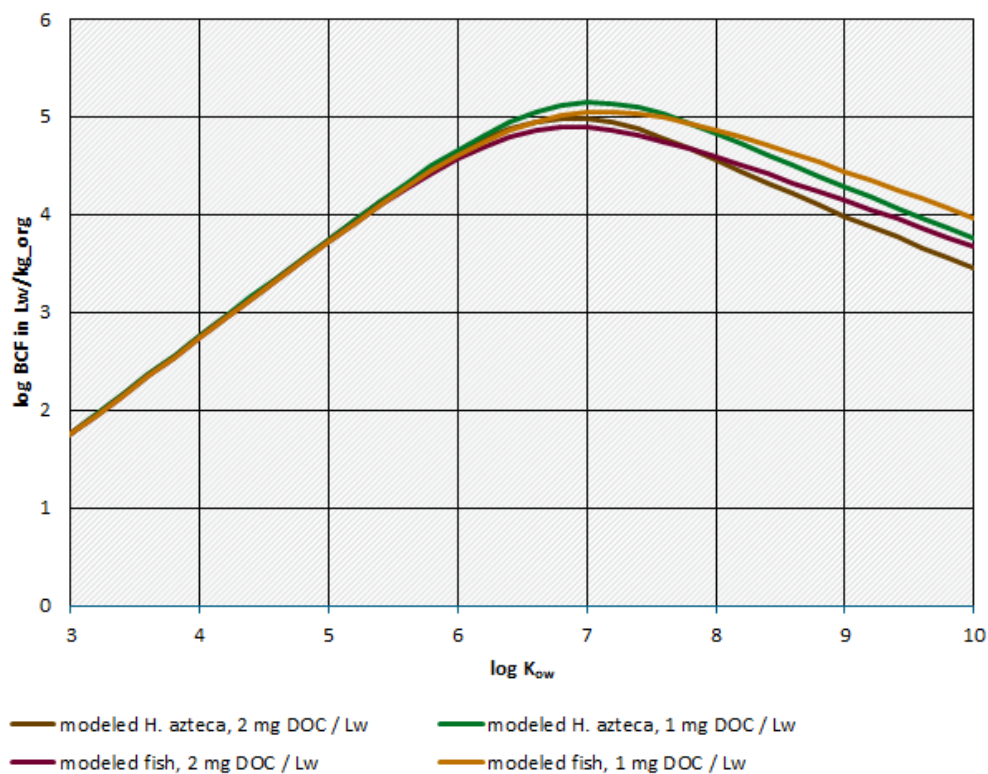
<https://echa.europa.eu/de/registration-dossier/-/registered-dossier/13220/5/4/2/?documentUUID=e0ac66f4-ba8f-461a-aaeb-0cd0f9f85aa2>. and REACH registration dossier for UV-234.

<https://echa.europa.eu/de/registration-dossier/-/registered-dossier/11135/5/4/2/?documentUUID=617b9e9b-a098-4a72-ad57-5cc5d53deed8>). In fish, both deducted BCF in fish are quite similar, the trend is even reversed, with log BCF of 2.6 (UV-329) and 3.0 (UV-234). Differences in k_2 might be explainable with different metabolic rates in *Hyalella azteca* and fish, yet the differences in k_1 have the most impact. Uptake rate constant k_1 of UV-329 is below model expectations by more than an order of magnitude. We believe this to be an experimental artifact, as in that experiment there were problems maintaining solute concentration, resulting in an extreme intermediate drop in internal body concentration. Also, steady state was never reached. We thus deem the fitted k_1 value unreliable. Additionally, for the uptake phase of UV-234 the TOC content reached up to 10 mg / L_w , well above the limit set by the OECD guideline 305 of 2 mg TOC / L_w . These fish experiments are therefore not suitable for showing a systematic difference between *Hyalella azteca* and fish.

To validate model predictions and confirm comparability between measurements in *Hyalella azteca* and fish of chemicals in the superhydrophobic range, still more experimental data will be needed, ideally measured both for *Hyalella azteca* and fish as test organism.

Modeling of k_1 , k_2 , or BCF for *Hyalella azteca* is still less reliable than for fish, simply due to less reliable physiological data and the sparse experimental values with which to test the model. Nevertheless, we believe the test with *Hyalella azteca* to have many experimental advantages, such as the smaller size of test system, lower medium consumption, or need for less test substance (Schlechtriem *et al.*, 2019). For superhydrophobic substances, three advantages stand out: i) The estimated k_2 rate constants (in the absence of metabolism and ignoring growth) are much higher for *Hyalella azteca* than for fish (see Appendix A.5), which should result in shorter required uptake periods, as has been reported by (Schlechtriem *et al.*, 2019), and ii) reduce the influence of growth, which was negligible for UV-234 and UV-329 (Schlechtriem *et al.*, 2021). Growth correction per se is deemed unreliable (Gobas and Lee, 2019), yet will be even more problematic if growth rate is in the same order of magnitude as (or even faster than) k_2 , a realistic scenario for superhydrophobic chemicals, that is for example reached in the fish test for UV-234; iii) due to the reduced biomass and smaller experimental setup, it should be easier to keep the TOC level below the threshold of 2 mg/L accepted by regulators, which has a high impact on k_1 for superhydrophobic compounds.

Figure 18: Log BCF in *Hyalella azteca* and in fish



Modeled BCF for (super)hydrophobic chemicals in *Hyalella azteca* and in fish. The values were calculated for an organism with 5% lipid content, for chemicals with MW of 400 g/mol in the presence of DOC as marked. For fish (trout), a feeding rate of 2% of body weight per day was assumed. Modeling was done using physiological data as stated in Table 1, not considering the effect of bloodflow.

Source: own illustration, Helmholtz Centre for Environmental Research GmbH - UFZ

3.4 Limits of applicability

In the absence of metabolism, for superhydrophobic compounds, the required duration of the uptake period will exceed realistic times for standard testing, see section 3.1. At log K_{ow} 7, already one month will be required to reach 90% of steady state.

There is also a general problem with the BCF for superhydrophobic compounds per se: By feeding an uncontaminated diet, an unrealistic additional elimination path is introduced, which would in reality always be accompanied by an uptake of contaminated food. As a result, BCF decrease with high log K_{ow}, and chemicals may be classified as less bioaccumulative than chemicals with lower log K_{ow} (or not bioaccumulative at all), even in the absence of metabolism.

Take away messages

- ▶ Experimental rate constants measured in H. Azteca for superhydrophobic compounds is plausible, but still more data are needed for validation.
 - Both, experiment and model, show increased k_1 and k_2 in H. azteca as compared to fish.
 - Both, experiment and model, show a decrease in k_1 and BCF with increasing $\log K_{ow}$ for superhydrophobic chemicals, the reasons being binding to TOC and elimination via feces, according to the model. This is only valid if nominal concentrations are used in the determination of k_1 . If only freely dissolved concentrations are used, k_1 should not decrease with increasing $\log K_{ow}$.
 - Both UV-234 and UV-329 would have to be classified as very bioaccumulative if only freely dissolved concentrations (not bound to TOC) were used in the determination of the BCF.

- ▶ Although shorter times till steady state are expected in H. Azteca than in fish due to the higher k_2 , in the absence of metabolism, for $\log K_{ow} > 7$, more than a month is expected until steady state is reached, exceeding standard test times.
- ▶ A group contribution approach to predicting fish biotransformation half-lives (Brown *et al.*, 2012) showed promising potential to predict significant metabolic activity in H. azteca, but still more data are needed for validation. Both elimination rate constants of UV-234 and UV-329 seem to be dominated by metabolism. Yet, it has to be kept in mind that this assumption is not rooted in experiment, but an empirical prediction, and therefore uncertain.
- ▶ Uncertainties in the prediction especially of $\log K_{ow}$ for superhydrophobic chemicals can lead to strong variations in the predictions.
- ▶ The standard BCF test is conceptually questionable as an evaluation criterion for the bioaccumulation of superhydrophobic substances for chemicals with a $\log K_{ow}$ above 6.5, because in that case, uncontaminated diet will not contribute to overall uptake, but elimination via feces will be significant. Thus, the BCF test will underestimate the bioaccumulative potential of superhydrophobic chemicals.
- ▶ An alternative that is in line with the original concept of BCF and that would work for superhydrophobic substances could be to combine estimated k_1 and k_2 for uptake and elimination via gills with $k_{metabolism}$ from in vitro experiments, to estimate the BCF without the influence of diet/feces.

4 List of references

- Annot, J.A. and Gobas, F.A.P.C. (2004) A food web bioaccumulation model for organic chemicals in aquatic ecosystems. *Environ. Toxicol. Chem.*, **23**, 2343–2355.
- Avdeef, A. (2010) Leakiness and Size Exclusion of Paracellular Channels in Cultured Epithelial Cell Monolayers– Interlaboratory Comparison. *Pharm. Res.*, **27**, 480–489.
- Barker Jørgensen, C., Møhlenberg, F., and Sten-Knudsen, O. (1986) Nature of relation between ventilation and oxygen consumption in filter feeders. *Mar. Ecol. Prog. Ser.*, **29**, 73–88.
- Bittermann, K. and Goss, K.U. (2017) Predicting apparent passive permeability of Caco-2 and MDCK cell-monolayers: A mechanistic model. *PLoS One*, **12**, 1–20.
- Böhm, L., Schlechtriem, C., and Düring, R.A. (2016) Sorption of Highly Hydrophobic Organic Chemicals to Organic Matter Relevant for Fish Bioconcentration Studies. *Environ. Sci. Technol.*, **50**, 8316–8323.
- Brown, T.N., Annot, J.A., and Wania, F. (2012) Iterative fragment selection: A group contribution approach to predicting fish biotransformation half-lives. *Environ. Sci. Technol.*, **46**, 8253–8260.
- Buddington, R.K. and Diamond, J.M. (1987) Pyloric ceca of fish: A ‘new’ absorptive organ. *Am. J. Physiol. - Gastrointest. Liver Physiol.*, **252**.
- Burkhard, L.P. (2000) Estimating dissolved organic carbon partition coefficients for nonionic organic chemicals. *Environ. Sci. Technol.*, **34**, 4663–4668.
- Depledge, M.H. and Bjerregaard, P. (1989) Haemolymph protein composition and copper levels in decapod crustaceans. *Helgoländer Meeresuntersuchungen*, **43**, 207–223.
- EAS-E Suite (Ver.0.95 - BETA; release Feb.; 2022). www.eas-e-suite.com. Accessed [2022-03-24].; Toronto; ON; Canada.
- Eckert, F. and Klamt, A. (2002) Fast solvent screening via quantum chemistry: COSMO-RS approach. *AIChE J.*, **48**, 369–385.
- Endo, S. and Goss, K.U. (2011) Serum albumin binding of structurally diverse neutral organic compounds: Data and models. *Chem. Res. Toxicol.*, **24**, 2293–2301.
- Erickson, R.J. and McKim, J.M. (1990) A model for exchange of organic chemicals at fish gills: flow and diffusion limitations. *Aquat. Toxicol.*, **18**, 175–197.
- Escher, B.I. *et al.* (2011) Protein and lipid binding parameters in rainbow trout (*Oncorhynchus mykiss*) blood and liver fractions to extrapolate from an in vitro metabolic degradation assay to in vivo bioaccumulation potential of hydrophobic organic chemicals. *Chem. Res. Toxicol.*, **24**, 1134–1143.
- Everitt, S., MacPherson, S., Brinkmann, M., Wiseman, S., and Pyle, G. (2020) Effects of weathered sediment-bound dilbit on freshwater amphipods (*Hyalella azteca*). *Aquat. Toxicol.*, **228**, 105630.
- Fitzpatrick, C.M. (1968) The population dynamics and bioenergetics of the isopod *Asellus aquaticus* L. in a small freshwater pond.
- Fredrick, W.S. and Ravichandran, S. (2012) Hemolymph proteins in marine crustaceans. *Asian Pac. J. Trop. Biomed.*, **2**, 496–502.
- Gaigalas, A.K., Hubbard, J.B., McCurley, M., and Woo, S. (1992) Diffusion of bovine serum albumin in aqueous solutions. *J. Phys. Chem.*, **96**, 2355–2359.
- Gauthier, P.T., Norwood, W.P., Prepas, E.E., and Pyle, G.G. (2016) Behavioural alterations from exposure to Cu, phenanthrene, and Cu-phenanthrene mixtures: Linking behaviour to acute toxic mechanisms in the aquatic amphipod, *Hyalella azteca*. *Aquat. Toxicol.*, **170**, 377–383.
- Gobas, F.A.P.C. and Lee, Y.S. (2019) Growth-Correcting the Bioconcentration Factor and Biomagnification Factor in Bioaccumulation Assessments. *Environ. Toxicol. Chem.*, **38**, 2065–2072.
- Halcrow, K. (2001) Ultrastructural features of the funnel of *Gammarus oceanicus* (Amphipoda). *J. Crustac. Biol.*, **21**, 631–639.

- Hansch, C., Leo, A., and Hoekman, D.H. (1995) Exploring QSAR.: Hydrophobic, electronic, and steric constants American Chemical Society.
- Hughes, G.M. (1970) A comparative approach to fish respiration. *Experientia*, **26**, 113–122.
- Johnke, R. (1973) The influence of season upon the oxygen consumption of two populations of the freshwater amphipod *hyalella azteca*. *Master thesis, Calif. State Univ. Fresno*.
- Kampfraath, A.A., Hunting, E.R., Mulder, C., Breure, A.M., Gessner, M.O., Kraak, M.H.S., and Admiraal, W. (2012) DECOTAB: A multipurpose standard substrate to assess effects of litter quality on microbial decomposition and invertebrate consumption. *Freshw. Sci.*, **31**, 1156–1162.
- Kelly, B.C., Gobas, F.A.P.C., and McLachlan, M.S. (2004) Intestinal absorption and biomagnification of organic contaminants in fish, wildlife, and humans. *Environ. Toxicol. Chem.*, **23**, 2324–2336.
- Kopinke, F.D., Ramus, K., Poerschmann, J., and Georgi, A. (2011) Kinetics of desorption of organic compounds from dissolved organic matter. *Environ. Sci. Technol.*, **45**, 10013–10019.
- Krause, S., Ulrich, N., and Goss, K.U. (2018) Desorption kinetics of organic chemicals from albumin. *Arch. Toxicol.*, **92**, 1065–1074.
- Larisch, W. (2019) Entwicklung eines PbTk-Modells für Wirbeltiere. *Diss. Martin-Luther-Universität Halle-wittenb.*
- Larisch, W. and Goss, K.U. (2018a) Modelling oral up-take of hydrophobic and super-hydrophobic chemicals in fish. *Environ. Sci. Process. Impacts*, **20**, 98–104.
- Larisch, W. and Goss, K.U. (2018b) Modelling oral up-take of hydrophobic and super-hydrophobic chemicals in fish. *Environ. Sci. Process. Impacts*, **20**, 98–104.
- Liu, L., Wu, F., Haderlein, S., and Grathwohl, P. (2013) Determination of the subcooled liquid solubilities of PAHs in partitioning batch experiments. *Geosci. Front.*, **4**, 123–126.
- Lorenzon, S., Martinis, M., and Ferrero, E.A. (2011) Ecological Relevance of Hemolymph Total Protein Concentration in Seven Unrelated Crustacean Species from Different Habitats Measured Predictively by a Density-Salinity Refractometer. *J. Mar. Biol.*, **2011**, 1–7.
- De Maagd, P.G.J., Ten Hulscher, D.T.H.E.M., Van Den Heuvel, H., Opperhuizen, A., and Sijm, D.T.H.M. (1998) Physicochemical properties of polycyclic aromatic hydrocarbons: Aqueous solubilities, n-octanol/water partition coefficients, and Henry's law constants. *Environ. Toxicol. Chem.*, **17**, 251–257.
- McCarthy, J.F. and Jimenez, B.D. (1985) Interactions between Polycyclic Aromatic Hydrocarbons and Dissolved Humic Material: Binding and Dissociation. *Environ. Sci. Technol.*, **19**, 1072–1076.
- Minghetti, M., Drieschner, C., Bramaz, N., Schug, H., and Schirmer, K. (2017) A fish intestinal epithelial barrier model established from the rainbow trout (*Oncorhynchus mykiss*) cell line, RTgutGC. *Cell Biol. Toxicol.*, **33**, 539–555.
- Morgan, M. (1971) Gill development, growth and respiration in the trout, *Salmo gairdneri* (Richardson).
- Nichols, J.W., McKim, J.M., Lien, G.J., Hoffman, A.D., Bertelsen, S.L., and Elonen, C.M. (1996) A physiologically based toxicokinetic model for dermal absorption of organic chemicals by fish. *Fundam. Appl. Toxicol.*, **31**, 229–242.
- Othman, M.S. and Pascoe, D. (2001) Growth, development and reproduction of *Hyalella Azteca* (Saussure, 1858) in laboratory culture. *Crustaceana*, **74**, 171–181.
- Rameshkumar, G., Ravichandran, S., Kaliyavarathan, G., and Ajithkumar, T.T. (2009) Comparison of Protein Content in the Haemolymph of Brachyuran Crabs. *In Vivo (Brooklyn)*, **4**, 32–35.
- Regan, S., Hynds, P., and Flynn, R. (2017) An overview of dissolved organic carbon in groundwater and implications for drinking water safety. *Hydrogeol. J.*, **25**, 959–967.
- Schlechtriem, C., Kampe, S., Bruckert, H.J., Bischof, I., Ebersbach, I., Kosfeld, V., Kotthoff, M., Schäfers, C., and L'Haridon, J. (2019) Bioconcentration studies with the freshwater amphipod *Hyalella azteca*: are the results predictive of bioconcentration in fish? *Environ. Sci. Pollut. Res.*, **26**, 1628–1641.

- Schlechtriem, C., Kühn, S., and Müller, C. (2021) Development of a bioaccumulation test using *Hyalella azteca* ; final report; project of the Umweltbundesamt, conducted by Fraunhofer Institute for Molecular Biology and Applied Ecology (Fraunhofer IME).
- Sushko, I. *et al.* (2011) Online chemical modeling environment (OCHEM): Web platform for data storage, model development and publishing of chemical information. *J. Comput. Aided. Mol. Des.*, **25**, 533–554.
- SUTCLIFFE, D.W. (1984) Quantitative aspects of oxygen uptake by *Gammarus* (Crustacea, Amphipoda): a critical review. *Freshw. Biol.*, **14**, 443–489.
- Trowell, J.J., Gobas, F.A.P.C., Moore, M.M., and Kennedy, C.J. (2018) Estimating the Bioconcentration Factors of Hydrophobic Organic Compounds from Biotransformation Rates Using Rainbow Trout Hepatocytes. *Arch. Environ. Contam. Toxicol.*, **75**, 295–305.
- Ulrich, N., Endo, S., Brown, T.N., Watanabe, N., Bronner, G., Abraham, M.H., and Goss, K.U. (2017) UFZ-LSER database v 3.2 [Internet].
- Walter, A. and Gutknecht, J. (1986) Permeability of small nonelectrolytes through lipid bilayer membranes. *J. Membr. Biol.*, **90**, 207–217.
- Welton, J.S., Ladle, M., Bass, J.A.B., and John, I.R. (1983) Estimation of Gut Throughput Time in *Gammarus Pulex* under Laboratory and Field Conditions with a Note on the Feeding of Young in the Brood Pouch. *Oikos*, **41**, 133.
- Westergaard, H. and Dietschy, J.M. (1976) The mechanism whereby bile acid micelles increase the rate of fatty acid and cholesterol uptake into the intestinal mucosal cell. *J. Clin. Invest.*, **58**, 97–108.
- de Wolf, W. *et al.* (2007) Animal use replacement, reduction, and refinement: development of an integrated testing strategy for bioconcentration of chemicals in fish. *Integr. Environ. Assess. Manag.*, **3**, 3–17.

A Appendix

A.1 DOC

To calculate the facilitation factor in water, only the presence of DOC was assumed (flow-through system, more than 90 % of TOC in water sources is reported to be DOC (Regan *et al.*, 2017)), and DOC/water partition coefficients were calculated using Equation (A1):

$$K_{DOC/water} = 0.08 * K_{ow} \quad (A1)$$

We did not find explicit methods to estimate DOC binding rate constants, but experimental desorption rate constants (Kopinke *et al.*, 2011) were lower by a factor of 30 than estimated albumin binding rate constants (Krause *et al.*, 2018). In a very rough estimate, we thus assumed the DOC desorption rate constant to be:

$$k_{des,DOC} = \frac{k_{des,ALB}}{30} = 20267 * MW_{chemical}^{-2}/30 \quad (A2)$$

Where $MW_{chemical}$ is the chemical's molecular weight in g/mol, k_{des} is the desorption rate constant in 1/s.

The relation between solute bound to DOC $m_{bound,DOC}$ and solute freely dissolved in water $m_{unbound}$ in equilibrium can be expressed as:

$$\frac{m_{bound,DOC}}{m_{unbound}} = \frac{k_{sorb,DOC}}{k_{des,DOC}} = K_{DOC/water} * c_{DOC} \quad (A3)$$

With $K_{DOC/water}$ being the DOC/water partition coefficient, c_{DOC} being the concentration of DOC in water, and $k_{sorb,DOC}$ being the sorption rate constant to DOC in 1/s.

$$k_{sorb,DOC} = K_{DOC/water} * c_{DOC} * k_{des,DOC} \quad (A4)$$

To estimate the influence of facilitated transport by DOC, compound both freely dissolved in water and bound to DOC must be considered separately. Transport rate constants for the diffusion through the ABL in water are different for the bound chemical, because their transport is limited by the diffusion of the carrier instead of the free chemical:

$$k_{ABL,bound} = \frac{D_{carrier} * A}{d_{ABL}} / M_{org} \quad (A5)$$

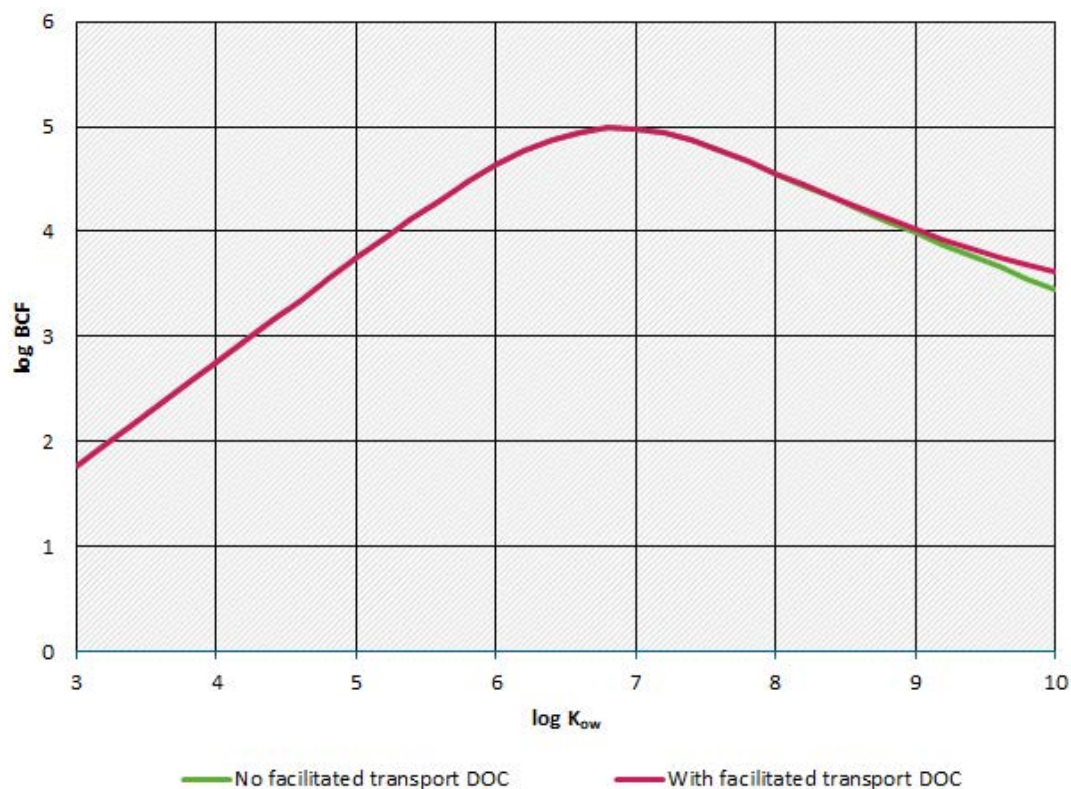
With $D_{carrier}$ being the diffusion constant of the carrier. DOC was assumed to be composed of humic acids, and a molecular weight of 1000 g/mol was used for the calculation of the diffusion constant according to Equation (8), resulting in $3.2 * 10^{-6} \text{ cm}^2/\text{s}$.

The system of equations in Table 3 was thus adapted to separately consider the unbound and bound chemical, and to allow for sorption and desorption processes in each aqueous volume, see Table 5. Additionally, the ABL was separated into 10 layers (not depicted in Table 5). It is needed to split the ABL in different layers, as de-/sorption processes take place during the whole diffusion process. A molecule only carried the last little stretch of the way will not contribute the same way to the facilitation factor as a molecule picked up from the start. For an ABL of 5 μm , the arising difference between 1 and 10 layers was the factor of 2. In the main model, facilitated transport was in the end not considered, due to the strong uncertainties in predicting k_{des} , and also because the effect did not seem to be very significant with the used k_{des} , see Figure 19.

Table 5: System of equations gills considering de-/sorption kinetics

| Equation | $C_{vent,unbound}$ | $C_{vent,bound}$ | $C_{ABL,gill,unbound}$ | $C_{ABL,gill,bound}$ | $C_{ABL,blood}$ | C_{org} | |
|----------|--|---|---|--|---|-------------------------------|--------------------------------------|
| I | - k_{vent} - $k_{ABL,w,unbound}$ - $k_{sorb} * V_{vent} / M_{org}$ | + $k_{des} * V_{vent} / M_{org}$ | + $k_{ABL,w,unbound}$ | 0 | 0 | 0 | - $f_{unbound} * k_{vent} * C_w$ |
| II | + $k_{sorb} * V_{vent} / M_{org}$ | - $k_{ABL,w,bound}$ - $k_{des} * V_{vent} / M_{org}$ | 0 | + $k_{ABL,w,bound}$ | 0 | 0 | - $(1-f_{unbound}) * k_{vent} * C_w$ |
| III | + $k_{ABL,w,unbound}$ | 0 | - $k_{ABL,w,unbound}$ - $k_{cell,gills}$ - $k_{sorb} * V_{ABL,w} / M_{org}$ | + $k_{des} * V_{ABL,w} / M_{org}$ | + $k_{cell,gills}$ | 0 | 0 |
| IV | 0 | + $k_{ABL,w,bound}$ | + $k_{sorb} * V_{ABL,w} / M_{org}$ | - $k_{ABL,w,bound}$ - $k_{des} * V_{ABL,w} / M_{org}$ | 0 | 0 | 0 |
| V | 0 | 0 | + $k_{cell,gills}$ | 0 | - $k_{cell,gills}$ - $k_{ABL,blood}$ | + $k_{ABL,blood} / K_{org/w}$ | 0 |
| VI | 0 | 0 | 0 | 0 | + $k_{ABL,blood}$ | - $k_{ABL,blood} / K_{org/w}$ | - Φ |

$f_{unbound}$ unbound fraction, k_{vent} ventilation rate constant, V_{vent} the ventilation volume, $V_{ABL}=A*d_{ABL}$ the volume of the ABL-layer, $k_{ABL,w,unbound} / k_{ABL,w,bound}$ rate constant for diffusion in aqueous ABL adjacent to gills for freely dissolved chemical/chemical bound to DOC, $k_{cell,gills}$ rate constant for diffusion through cell monolayer, $k_{ABL,blood}$ rate constant for diffusion through ABL in blood, Φ the resulting flux, C_{vent} is the concentration in the ventilation volume, $C_{ABL,gills}$ is the concentration in the aqueous ABL adjacent to the gill membrane, $C_{ABL,blood}$ is the concentration in the blood ABL adjacent to the gill cells, C_{org} is the concentration in the organism, at equilibrium with the blood, C_w is the concentration in water.

Figure 19: Influence of facilitated transport with DOC on log BCF


Modeled BCF for (super)hydrophobic chemicals, including or excluding facilitated transport with DOC as carrier in water. The values were calculated for a 3 mg organism with 5% lipid content. Modeling was done in the presence of 2 mg DOC/L_w for chemicals with MW of 400 g/mol and in the absence of metabolism.

Source: own illustration, Helmholtz Centre for Environmental Research GmbH - UFZ

A.2 Facilitation factor in blood

To calculate the facilitation factor in blood, albumin-like proteins with similar binding properties were assumed to be present at the same concentration as in fish. Albumin/water partition coefficients were either calculated using LSERD (Ulrich *et al.*, 2017) with experimental descriptors, or the following correlation to the log K_{ow} (Endo and Goss, 2011):

$$K_{ALB/water} = 0.71 * \log K_{ow} + 0.42 \quad (A6)$$

The desorption rate from albumin can be calculated from an empirical correlation to the chemical's molecular weight according to Equation (12) (Krause *et al.*, 2018):

$$k_{des,ALB} = 20267 * MW_{chemical}^{-2} \quad (A7)$$

Where MW_{chemical} is the chemical's molecular weight in g/mol, k_{des} is the desorption rate constant in 1/s.

The relation between solute bound to albumin $m_{bound,ALB}$ and solute freely dissolved in water m_{free} in equilibrium can be expressed as:

$$\frac{m_{bound,ALB}}{m_{free}} = \frac{k_{sorb,ALB}}{k_{des,ALB}} = K_{ALB/water} * c_{ALB} \quad (A8)$$

With $K_{ALB/water}$ being the albumin/water partition coefficient, c_{ALB} being the concentration of albumin in water, and $k_{sorb,ALB}$ being the sorption rate constant to albumin in 1/s.

$$k_{sorb,ALB} = K_{ALB/water} * c_{ALB} * k_{des,ALB} \tag{A9}$$

To estimate the influence of facilitated transport by albumin in blood, compound both freely dissolved in water and bound to albumin must be considered separately. Only the fraction unbound can move across cell membranes, but both fractions may traverse the unstirred water layer in blood (or be transported via bloodflow, which is not considered here). Transport rate constants for the diffusion through the ABL in blood are different for the bound chemical, because their transport is limited by the diffusion of the carrier instead of the free chemical:

$$k_{ABL,bound} = \frac{D_{carrier} * A}{d_{ABL}} / M_{org} \tag{A10}$$

With $D_{carrier}$ being the diffusion constant of the carrier, in this case albumin.

Additionally, the ABL was separated into 10 layers. It is needed to split the ABL in different layers, as de-/sorption processes take place during the whole diffusion process. A molecule only carried the last little stretch of the way will not contribute the same way to the facilitation factor as a molecule picked up from the start. For an ABL of 286 nm, the arising difference between 1 and 10 layers was the factor of 10.

Solving the system of equations in Table 6 and comparing the resulting flux to the diffusion of the free species alone, we can calculate a facilitation factor (results listed in Table 7 and 8). The resulting facilitation factors FAC were then used to calculate the rate constant of diffusion through the ABL in blood:

$$k_{ABL,blood} = FAC * k_{ABL,blood,unbound} = FAC * \frac{D_{chemical} * A}{d_{ABL}} / M_{org} \tag{A11}$$

Where $D_{chemical}$ is the diffusion constant of the chemical and d_{ABL} the total thickness of the ABL.

Table 6: System of equations considering de-/sorption kinetics to calculate FAC in blood

| Equation | Cabl_blood, free, layer1 | Cabl_blood, bound, layer1 | Cabl_blood, free, layer2 | Cabl_blood, bound, layer2 | layers 3...10 | Cblood,free | Cblood,bound | |
|----------|---|--|---|--|---------------|-------------|--------------|------------------------------|
| I | - k_{cell} $k_{ABL,blood,unbound} - k_{sorb} * V_{bloodlayer} / M_{org}$ | + $k_{des} * V_{bloodlayer} / M_{org}$ | + $k_{ABL,blood,unbound}$ | 0 | ... | 0 | 0 | - $k_{cell} * C_{w,unbound}$ |
| II | + $k_{sorb} * V_{bloodlayer} / M_{org}$ | - $k_{ABL,blood,bound} - k_{des} * V_{bloodlayer} / M_{org}$ | 0 | + $k_{ABL,blood,bound}$ | ... | 0 | 0 | 0 |
| | + $k_{ABL,blood,unbound}$ | 0 | - $2 * k_{ABL,blood,unbound} - k_{sorb} * V_{bloodlayer} / M_{org}$ | + $k_{des} * V_{bloodlayer} / M_{org}$ | ... | 0 | 0 | 0 |
| IV | 0 | + $k_{ABL,blood,bound}$ | + $k_{sorb} * V_{bloodlayer} / M_{org}$ | - $2 * k_{ABL,bound} - k_{des} * V_{bloodlayer} / M_{org}$ | ... | 0 | 0 | 0 |
| V-XX | ... | ... | ... | ... | ... | ... | ... | ... |

| Equation | C _{abl_blood, free, layer1} | C _{abl_blood, bound, layer1} | C _{abl_blood, free, layer2} | C _{abl_blood, bound, layer2} | layers 3...10 | C _{blood, free} | C _{blood, bound} | |
|----------|--------------------------------------|---------------------------------------|--------------------------------------|---------------------------------------|---------------|--|--|-----|
| XXI | 0 | 0 | 0 | 0 | ... | - k _{ABL, blood, unbound} * V _{ABL_blood} / M _{org} | + k _{des} * V _{blood} / M _{org} | - Φ |
| XXII | 0 | 0 | 0 | 0 | ... | + k _{sorb} * V _{blood} / M _{org} | - k _{ABL, bound} - k _{des} * V _{blood} / M _{org} | 0 |

$V_{\text{bloodlayer}} = A * d_{\text{ABL, blood, layer}} = A * d_{\text{ABL, blood}} / 10$ the volume of a single ABL-layer, $k_{\text{ABL, blood, unbound}} / k_{\text{ABL, blood, bound}}$ rate constant for diffusion in the ABL in blood for freely dissolved chemical/chemical bound to albumin-like proteins for one ABL layer of thickness $d_{\text{ABL}} / 10$, k_{cell} rate constant for diffusion through a cell monolayer, which is assumed extremely high (not limiting, as are all other processes except for the diffusion through blood) just for the calculations of the FAC, Φ the resulting flux, $c_{\text{w, unbound}}$ is the concentration in water of the unbound chemical.

A.3 Bile acids as carriers in the gut

The facilitated transport via bile acids in the gut was estimated according to (Westergaard and Dietschy, 1976; Larisch and Goss, 2018a; Larisch, 2019) from subcooled solubility:

$$FAC = 0.3972 * S_{\text{subcooled}}^{-0.584} \tag{A12}$$

Where $S_{\text{subcooled}}$ is the subcooled solubility in mM.

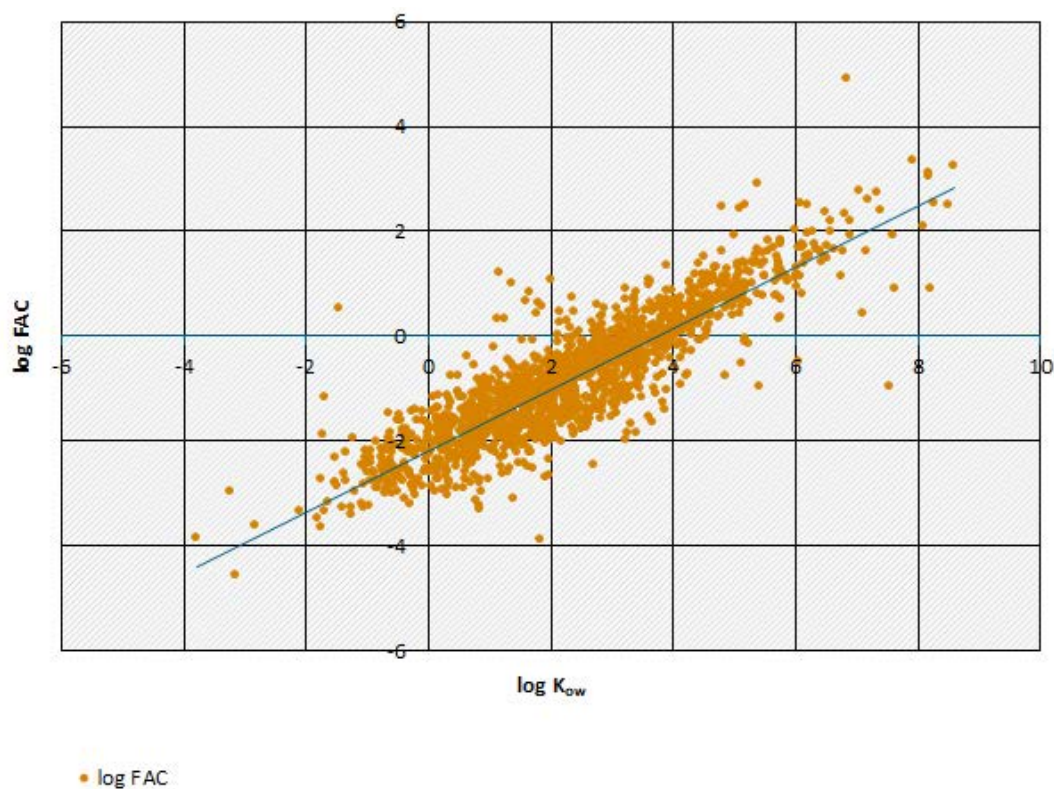
Which is calculated approximatively according to (Liu *et al.*, 2013) from aqueous solubility S_w and melting temperature T_m (in K), see Equation (A13):

$$S_{\text{subcooled}} = \frac{S_w}{\exp\left[\frac{T_m * \Delta S_m}{R * T_m} * \left(1 - \frac{T_m}{T}\right)\right]} / MW \tag{A13}$$

Where T is the temperature in Kelvin, R the gas constant, and ΔS_m the entropy of fusion with approximately 56.5 J/mol/K . The aqueous solubility S_w (in mg/L) was predicted using Episuite.

Please keep in mind that these predictions are quite uncertain, because the prediction model of the FAC by micellar transport is an empirical model based solely on fatty acids as input data. Also, while the FAC depends on $\log K_{ow}$, there is wide scatter, see Figure 20. The estimated FAC depending on $\log K_{ow}$ can thus only be considered as a rough estimate, and specific FACs should be calculated for specific chemicals for better results. For FAC below 1, FAC was set to 1.

Figure 20: Correlation between micelle facilitation factor and K_{ow}



Correlation between calculated log FAC and experimental log K_{ow} . Micelle facilitation factors were calculated at 297 K using Equations (A12) and (A13) for 1601 chemicals for which experimental log K_{ow} (Hansch *et al.*, 1995), experimental aqueous solubilities and experimental melting temperatures (QSAR Toolbox version 4.4.1, which is freely available on the OECD website (<http://www.qsartoolbox.org/>)) were available. Trendline: $\log FAC = 0.58 * \log K_{ow} - 2.18$.

Source: own illustration, Helmholtz Centre for Environmental Research GmbH - UFZ

A.4 Cell permeation

Although the permeability through cell membranes correlates to a higher degree to hexadecane/water than octanol/water partition coefficients (Walter and Gutknecht, 1986), for simplicity an empirical correlation between membrane permeability P_{mem} for neutral compounds and the octanol/water partition coefficient will be used to P_{mem} (Walter and Gutknecht, 1986):

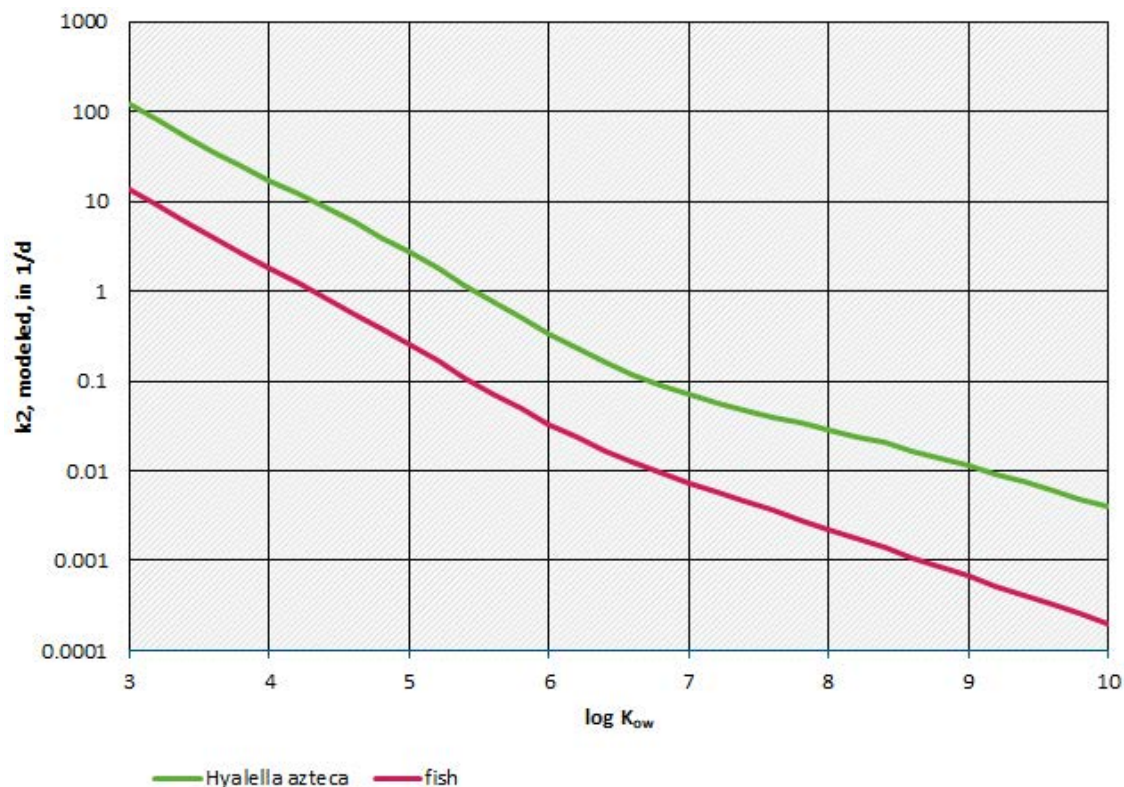
$$\log P_{mem} = 1.15 * \log K_{ow} - 2.14 \quad (A14)$$

With P_{mem} in cm/s, with $P_{mem} = 1 / R_{mem}$.

Lateral transport and cytosolic transport are calculated as described in detail in (Bittermann and Goss, 2017).

A.5 Comparison of modeled rate constant k2 in H. azteca and fish

Figure 21: Comparison of modeled rate constant k2 in H. azteca and fish



Modeled rate constant k2 in H. Azteca and fish depending on log K_{ow}. Rate constant k2 was calculated for a 3 mg organism with 2% lipid content for H. azteca, and a 2.2 g rainbow trout with 3.7% lipid content, respectively. The modeling was done for a compound with MW of 400 g/mol, assuming no metabolism.

Source: own illustration, Helmholtz Centre for Environmental Research GmbH – UFZ

A.6 Tabular data

Table 7: Diffusion coefficient D_w, albumin/water partition coefficient K_{albumin/w}, aqueous solubility S_w, melting temperature T_m, subcooled solubility S_{subcooled}, calculated facilitation factors by bile micelles in the gut FAC_{mic} and albumin in blood FAC_{albumin} for hydrophobic chemicals

| Chemical | D _w (cm ² /s) ^a | Log K _{albumin/w} ^b | S _w (mg/L) | T _m (°C) ^c | S _{subcooled} (mg/L) ^d | FAC _{mic} ^e | FAC _{albumin} ^f |
|-------------------|--|---|-----------------------|----------------------------------|--|---------------------------------|-------------------------------------|
| UV-234 | 4.7E-06 | 7.31 | 1.65E-03 ^g | 139 | 2.36E-02 | 125 | 3.2 |
| UV-329 | 5.4E-06 | 6.05 | 1.68E-01 ^g | 106 | 1.13E+00 | 11 | 1.3 |
| hexachlorobenzene | 5.73E-06 | 4.64 | 4.70E-03 ^c | 229 | 5.29E-01 | 16 | 1.0 |
| ortho-terphenyl | 6.31E-06 | 4.84 | 1.24E+00 ^c | 56 | 2.66E+00 | 5 | 1.0 |
| benzo(a)pyrene | 6.05E-06 | 5.15 | 1.62E-03 ^c | 179 | 5.81E-02 | 53 | 1.0 |

| Chemical | D _w (cm ² /s) ^a | Log K _{albumin/w} ^b | S _w (mg/L) | T _m (°C) ^c | S _{subcooled} ^d (mg/L) | FAC _{mic} ^e | FAC _{albumin} ^f |
|--------------|--|---|-----------------------|----------------------------------|--|---------------------------------|-------------------------------------|
| PCB153 | 5.15E-06 | 6.05 | 9.49E-04 ^c | 103 | 5.95E-03 | 247 | 1.2 |
| PCB77 | 5.66E-06 | 5.35 | 1.80E-01 ^c | 182 | 6.92E+00 | 4 | 1.1 |
| chlorpyrifos | 5.21E-06 | 3.40 | 1.12E+00 ^c | 42 | 1.73E+00 | 9 | 1.0 |
| methoxychlor | 5.25E-06 | 4.63 | 9.99E-02 ^c | 87 | 2.30E-02 | 20 | 1.0 |
| pyrene | 6.69E-06 | 4.40 | 1.35E-01 ^c | 151 | 7.16E-03 | 5 | 1.0 |

^a predicted according to Equation (8), ^b predicted using LSERD (Ulrich *et al.*, 2017), ^c experimental values taken from Pubchem <https://pubchem.ncbi.nlm.nih.gov/>, ^d predicted using Equation (A13), ^e predicted using Equation (A12), ^f predicted for ABL blood thickness of 286 nm and albumin mass fraction of 41.2 g/L_{plasma}, ^g predicted using Episuite.

Table 8: Calculated facilitation factors by bile micelles in the gut FAC_{mic} and albumin in blood FAC_{albumin} depending on the octanol/water partition coefficient log K_{ow}

| Log K _{ow} | FAC _{mic} ^a | FAC _{albumin} ^b | Log K _{ow} | FAC _{mic} ^a | FAC _{albumin} ^b |
|---------------------|---------------------------------|-------------------------------------|---------------------|---------------------------------|-------------------------------------|
| 3 | 1 | 1.0 | 6.6 | 44 | 1.0 |
| 3.2 | 1 | 1.0 | 6.8 | 58 | 1.0 |
| 3.4 | 1 | 1.0 | 7 | 76 | 1.1 |
| 3.6 | 1 | 1.0 | 7.2 | 99 | 1.1 |
| 3.8 | 1 | 1.0 | 7.4 | 129 | 1.1 |
| 4 | 1 | 1.0 | 7.6 | 169 | 1.1 |
| 4.2 | 2 | 1.0 | 7.8 | 221 | 1.2 |
| 4.4 | 2 | 1.0 | 8 | 288 | 1.3 |
| 4.6 | 3 | 1.0 | 8.2 | 377 | 1.4 |
| 4.8 | 4 | 1.0 | 8.4 | 492 | 1.5 |
| 5 | 5 | 1.0 | 8.6 | 643 | 1.7 |
| 5.2 | 7 | 1.0 | 8.8 | 839 | 2.0 |
| 5.4 | 9 | 1.0 | 9 | 1096 | 2.3 |
| 5.6 | 12 | 1.0 | 9.2 | 1432 | 2.7 |
| 5.8 | 15 | 1.0 | 9.4 | 1871 | 3.2 |
| 6 | 20 | 1.0 | 9.6 | 2443 | 3.8 |
| 6.2 | 26 | 1.0 | 9.8 | 3192 | 4.6 |
| 6.4 | 34 | 1.0 | 10 | 4169 | 5.6 |

^a predicted using equation A12, ^b predicted for ABL blood thickness of 286 nm and albumin mass fraction of 41.2 g/L_{plasma}

Table 9: Predicted rate constants k1, k2 (not considering metabolism), k2m (considering metabolism), experimental rate constants k1exp and k2exp, predicted biotransformation half life

| Chemical | k1 (Lw/kg _{org} /d) | k2 (1/d) | k2 _m (1/d) | k1 _{exp} (Lw/kg _{org} /d) | k2 _{exp} (1/d) | half-life (h) |
|-------------------|---------------------------------|-------------|--------------------------|--|----------------------------|------------------|
| UV-234 | 2.70E+02 | 7.28E-03 | 1.06E-01 | 1.98E+02 | 2.73E-01 | 168.16 |
| UV-329 | 7.40E+03 | 1.36E-01 | 6.50E-01 | 8.29E+03 | 9.92E-01 | 32.33 |
| hexachlorobenzene | 8.98E+03 | 6.57E-01 | 7.14E-01 | 2.75E+03 | 4.17E-01 | 296.03 |
| ortho-terphenyl | 9.59E+03 | 6.67E-01 | 8.54E-01 | 1.22E+03 | 4.65E-01 | 88.78 |
| benzo(a)pyrene | 8.93E+03 | 3.05E-01 | 6.00E-01 | 6.66E+03 | 2.04E+00 | 56.38 |
| PCB153 | 1.64E+03 | 3.75E-02 | 3.91E-02 | 7.88E+03 | 7.90E-02 | 10522.54 |
| PCB77 | 6.72E+03 | 7.80E-02 | 9.00E-02 | 6.62E+03 | 1.64E-01 | 1387.17 |
| chlorpyrifos | 7.79E+03 | 3.06E+00 | 3.14E+00 | 4.34E+02 | 4.73E-01 | 64.7 |
| methoxychlor | 8.03E+03 | 2.41E+00 | 2.50E+00 | 4.95E+03 | 7.98E-01 | 201.23 |
| pyrene | 9.30E+03 | 4.36E+00 | 4.64E+00 | 4.19E+03 | 7.14E-01 | 59.24 |

Predictions were done for H. Azteca of 3 mg weight and 2% body fat content. Experimental rate constants taken from (Schlechtriem *et al.*, 2021) and (Schlechtriem *et al.*, 2019). Biotransformation half-life was predicted using (Brown *et al.*, 2012)(EAS-E Suite).

Table 10: Calculated log BCF (without consideration of metabolism), log BCF_m (considering metabolism), BCF_{exp_k2} (calculated using calculated k1 and experimental k2), and experimental BCF_{exp}

| Chemical | Log BCF ^a | Log BCF _m ^a | Log BCF _{exp_k2} ^b | Log BCF _{exp} ^c |
|-------------------|----------------------|-----------------------------------|--|-------------------------------------|
| UV-234 | 4.87 | 3.42 | 3.39 | 3.18 |
| UV-329 | 5.04 | 4.10 | 4.27 | 4.30 |
| hexachlorobenzene | 4.44 | 4.37 | 4.73 | 4.41 |
| ortho-terphenyl | 4.46 | 4.27 | 4.71 | 4.01 |
| benzo(a)pyrene | 4.77 | 4.30 | 4.04 | 3.81 |
| PCB153 | 4.94 | 4.91 | 4.71 | 5.41 |
| PCB77 | 5.24 | 5.12 | 5.01 | 5.01 |
| chlorpyrifos | 3.71 | 3.69 | 4.61 | 3.29 |
| methoxychlor | 3.83 | 3.80 | 4.40 | 3.79 |
| pyrene | 3.63 | 3.58 | 4.51 | 3.77 |

^a Predictions were done for 5% lipid content, ^b normalization was done for Log BCF_{exp_k2}, ^c experimental kinetic BCF (normalized to 5% lipid content) taken from (Schlechtriem *et al.*, 2021) and (Schlechtriem *et al.*, 2019).

Table 11: Hyalella Azteca: Calculated rate constants k1 for TOC content of 1 mg DOC/L and 2 mg DOC/L, respectively, k2 and estimated times till steady state, 50% and 90% respectively, depending on the octanol/water partition coefficient log K_{ow}

| Log K _{ow} | k1 {1 mg DOC/L} (L _w /k _{gorg} /d) | k1 {2 mg DOC/L} (L _w /k _{gorg} /d) | k2 (1/d) | T50 (d) | T90 (d) |
|---------------------|--|--|-------------|------------|------------|
| 3 | 3.48E+03 | 3.48E+03 | 2.93E+03 | 5.85E-03 | 1.94E-02 |
| 3.2 | 3.63E+03 | 3.63E+03 | 3.21E+03 | 8.81E-03 | 2.93E-02 |
| 3.4 | 3.83E+03 | 3.83E+03 | 3.30E+03 | 1.31E-02 | 4.36E-02 |
| 3.6 | 4.12E+03 | 4.12E+03 | 3.22E+03 | 1.93E-02 | 6.40E-02 |
| 3.8 | 4.50E+03 | 4.49E+03 | 2.98E+03 | 2.79E-02 | 9.26E-02 |
| 4 | 4.96E+03 | 4.96E+03 | 2.61E+03 | 3.99E-02 | 1.33E-01 |
| 4.2 | 5.50E+03 | 5.50E+03 | 2.16E+03 | 5.69E-02 | 1.89E-01 |
| 4.4 | 6.07E+03 | 6.06E+03 | 1.69E+03 | 8.15E-02 | 2.71E-01 |
| 4.6 | 6.63E+03 | 6.61E+03 | 1.25E+03 | 1.18E-01 | 3.92E-01 |
| 4.8 | 7.12E+03 | 7.08E+03 | 8.92E+02 | 1.73E-01 | 5.75E-01 |
| 5 | 7.51E+03 | 7.45E+03 | 6.13E+02 | 2.57E-01 | 8.55E-01 |
| 5.2 | 7.79E+03 | 7.70E+03 | 4.12E+02 | 3.88E-01 | 1.29E+00 |
| 5.4 | 7.97E+03 | 7.82E+03 | 2.73E+02 | 5.88E-01 | 1.95E+00 |
| 5.6 | 8.05E+03 | 7.80E+03 | 1.80E+02 | 8.93E-01 | 2.97E+00 |
| 5.8 | 8.02E+03 | 7.65E+03 | 1.19E+02 | 1.35E+00 | 4.48E+00 |
| 6 | 7.87E+03 | 7.33E+03 | 7.87E+01 | 2.02E+00 | 6.70E+00 |
| 6.2 | 7.59E+03 | 6.83E+03 | 5.28E+01 | 2.96E+00 | 9.83E+00 |
| 6.4 | 7.16E+03 | 6.13E+03 | 3.60E+01 | 4.23E+00 | 1.40E+01 |
| 6.6 | 6.54E+03 | 5.27E+03 | 2.49E+01 | 5.84E+00 | 1.94E+01 |
| 6.8 | 5.74E+03 | 4.30E+03 | 1.74E+01 | 7.76E+00 | 2.58E+01 |
| 7 | 4.81E+03 | 3.33E+03 | 1.22E+01 | 9.93E+00 | 3.30E+01 |
| 7.2 | 3.82E+03 | 2.45E+03 | 8.51E+00 | 1.23E+01 | 4.08E+01 |
| 7.4 | 2.88E+03 | 1.73E+03 | 5.88E+00 | 1.48E+01 | 4.91E+01 |
| 7.6 | 2.08E+03 | 1.18E+03 | 4.01E+00 | 1.75E+01 | 5.81E+01 |
| 7.8 | 1.44E+03 | 7.85E+02 | 2.69E+00 | 2.06E+01 | 6.83E+01 |
| 8 | 9.70E+02 | 5.13E+02 | 1.79E+00 | 2.42E+01 | 8.03E+01 |
| 8.2 | 6.40E+02 | 3.32E+02 | 1.18E+00 | 2.86E+01 | 9.49E+01 |

| Log K _{ow} | k1 {1 mg DOC/L} (L _w /k _{gorg} /d) | k1 {2 mg DOC/L} (L _w /k _{gorg} /d) | k2 (1/d) | T50 (d) | T90 (d) |
|---------------------|--|--|-------------|------------|------------|
| 8.4 | 4.16E+02 | 2.13E+02 | 7.76E-01 | 3.41E+01 | 1.13E+02 |
| 8.6 | 2.68E+02 | 1.36E+02 | 5.14E-01 | 4.10E+01 | 1.36E+02 |
| 8.8 | 1.71E+02 | 8.65E+01 | 3.44E-01 | 4.97E+01 | 1.65E+02 |
| 9 | 1.09E+02 | 5.49E+01 | 2.34E-01 | 6.06E+01 | 2.01E+02 |
| 9.2 | 6.94E+01 | 3.48E+01 | 1.64E-01 | 7.44E+01 | 2.47E+02 |
| 9.4 | 4.40E+01 | 2.21E+01 | 1.19E-01 | 9.17E+01 | 3.05E+02 |
| 9.6 | 2.79E+01 | 1.40E+01 | 8.93E-02 | 1.13E+02 | 3.77E+02 |
| 9.8 | 1.76E+01 | 8.83E+00 | 6.98E-02 | 1.41E+02 | 4.68E+02 |
| 10 | 1.12E+01 | 5.58E+00 | 5.65E-02 | 1.75E+02 | 5.82E+02 |

Predictions were done for H. Azteca of 3 mg weight and 2% body fat content.

Table 12: Fish: Calculated rate constants k1 for TOC content of 1 mg DOC/L and 2 mg DOC/L, respectively, k2 and estimated times till steady state, 50% and 90% respectively, depending on the octanol/water partition coefficient log K_{ow}

| Log K _{ow} | k1_DOC {1 mg DOC/L} (L _w /k _{gorg} /d) | k1 {2 mg DOC/L} (L _w /k _{gorg} /d) | k2 (1/d) | T50 (d) | T90 (d) |
|---------------------|--|--|-------------|------------|------------|
| 3 | 5.89E+02 | 5.89E+02 | 1.34E+01 | 5.16E-02 | 1.71E-01 |
| 3.2 | 6.09E+02 | 6.09E+02 | 8.83E+00 | 7.85E-02 | 2.61E-01 |
| 3.4 | 6.36E+02 | 6.36E+02 | 5.85E+00 | 1.18E-01 | 3.93E-01 |
| 3.6 | 6.73E+02 | 6.73E+02 | 3.92E+00 | 1.77E-01 | 5.87E-01 |
| 3.8 | 7.20E+02 | 7.20E+02 | 2.65E+00 | 2.61E-01 | 8.67E-01 |
| 4 | 7.76E+02 | 7.75E+02 | 1.81E+00 | 3.83E-01 | 1.27E+00 |
| 4.2 | 8.37E+02 | 8.36E+02 | 1.24E+00 | 5.61E-01 | 1.86E+00 |
| 4.4 | 8.98E+02 | 8.96E+02 | 8.41E-01 | 8.24E-01 | 2.74E+00 |
| 4.6 | 9.53E+02 | 9.50E+02 | 5.67E-01 | 1.22E+00 | 4.06E+00 |
| 4.8 | 1.00E+03 | 9.95E+02 | 3.79E-01 | 1.83E+00 | 6.07E+00 |
| 5 | 1.03E+03 | 1.03E+03 | 2.51E-01 | 2.76E+00 | 9.16E+00 |
| 5.2 | 1.06E+03 | 1.05E+03 | 1.66E-01 | 4.17E+00 | 1.39E+01 |
| 5.4 | 1.07E+03 | 1.05E+03 | 1.10E-01 | 6.32E+00 | 2.10E+01 |
| 5.6 | 1.07E+03 | 1.04E+03 | 7.29E-02 | 9.51E+00 | 3.16E+01 |
| 5.8 | 1.06E+03 | 1.01E+03 | 4.90E-02 | 1.41E+01 | 4.70E+01 |

| Log K _{ow} | k1_DOC {1 mg DOC/L} (L _w /k _{gorg} /d) | k1 {2 mg DOC/L} (L _w /k _{gorg} /d) | k2 (1/d) | T50 (d) | T90 (d) |
|---------------------|--|--|-------------|------------|------------|
| 6 | 1.04E+03 | 9.69E+02 | 3.35E-02 | 2.07E+01 | 6.87E+01 |
| 6.2 | 1.00E+03 | 9.00E+02 | 2.35E-02 | 2.96E+01 | 9.82E+01 |
| 6.4 | 9.42E+02 | 8.07E+02 | 1.68E-02 | 4.11E+01 | 1.37E+02 |
| 6.6 | 8.60E+02 | 6.93E+02 | 1.24E-02 | 5.57E+01 | 1.85E+02 |
| 6.8 | 7.55E+02 | 5.65E+02 | 9.42E-03 | 7.36E+01 | 2.45E+02 |
| 7 | 6.32E+02 | 4.37E+02 | 7.28E-03 | 9.52E+01 | 3.16E+02 |
| 7.2 | 5.02E+02 | 3.22E+02 | 5.72E-03 | 1.21E+02 | 4.03E+02 |
| 7.4 | 3.78E+02 | 2.27E+02 | 4.53E-03 | 1.53E+02 | 5.09E+02 |
| 7.6 | 2.72E+02 | 1.55E+02 | 3.59E-03 | 1.93E+02 | 6.41E+02 |
| 7.8 | 1.89E+02 | 1.03E+02 | 2.85E-03 | 2.43E+02 | 8.08E+02 |
| 8 | 1.27E+02 | 6.72E+01 | 2.25E-03 | 3.08E+02 | 1.02E+03 |
| 8.2 | 8.37E+01 | 4.34E+01 | 1.77E-03 | 3.92E+02 | 1.30E+03 |
| 8.4 | 5.43E+01 | 2.78E+01 | 1.38E-03 | 5.01E+02 | 1.66E+03 |
| 8.6 | 3.50E+01 | 1.78E+01 | 1.08E-03 | 6.40E+02 | 2.13E+03 |
| 8.8 | 2.23E+01 | 1.13E+01 | 8.46E-04 | 8.19E+02 | 2.72E+03 |
| 9 | 1.42E+01 | 7.16E+00 | 6.63E-04 | 1.05E+03 | 3.47E+03 |
| 9.2 | 9.03E+00 | 4.53E+00 | 5.20E-04 | 1.33E+03 | 4.42E+03 |
| 9.4 | 5.72E+00 | 2.87E+00 | 4.09E-04 | 1.69E+03 | 5.62E+03 |
| 9.6 | 3.62E+00 | 1.81E+00 | 3.23E-04 | 2.15E+03 | 7.13E+03 |
| 9.8 | 2.29E+00 | 1.15E+00 | 2.55E-04 | 2.72E+03 | 9.03E+03 |
| 10 | 1.45E+00 | 7.24E-01 | 2.02E-04 | 3.44E+03 | 1.14E+04 |

Predictions were done for rainbow trout of 2.2 g weight and 3.7% body fat content.

Table 13: log BCF in *H. Azteca* and fish, calculated for 1 mg DOC/L and 2 mg DOC/L, respectively, depending on the octanol/water partition coefficient log K_{ow}

| Log K _{ow} | Log BCF {1 mg DOC/L, <i>H. azteca</i> } | Log BCF {2 mg DOC/L, <i>H. azteca</i> } | Log BCF {1 mg DOC/L, fish} | Log BCF {2 mg DOC/L, fish} |
|---------------------|---|---|----------------------------------|----------------------------------|
| 3 | 1.77 | 1.77 | 1.75 | 1.75 |
| 3.2 | 1.96 | 1.96 | 1.95 | 1.95 |
| 3.4 | 2.16 | 2.16 | 2.15 | 2.15 |

| Log K _{ow} | Log BCF {1 mg DOC/L, H. azteca} | Log BCF {2 mg DOC/L, H. azteca} | Log BCF {1 mg DOC/L, fish} | Log BCF {2 mg DOC/L, fish} |
|---------------------|---------------------------------------|---------------------------------------|----------------------------------|----------------------------------|
| 3.6 | 2.36 | 2.36 | 2.35 | 2.35 |
| 3.8 | 2.56 | 2.56 | 2.54 | 2.54 |
| 4 | 2.76 | 2.76 | 2.74 | 2.74 |
| 4.2 | 2.96 | 2.96 | 2.94 | 2.94 |
| 4.4 | 3.16 | 3.16 | 3.14 | 3.14 |
| 4.6 | 3.36 | 3.35 | 3.34 | 3.33 |
| 4.8 | 3.55 | 3.55 | 3.53 | 3.53 |
| 5 | 3.75 | 3.75 | 3.73 | 3.72 |
| 5.2 | 3.94 | 3.94 | 3.92 | 3.91 |
| 5.4 | 4.13 | 4.12 | 4.10 | 4.09 |
| 5.6 | 4.32 | 4.31 | 4.28 | 4.27 |
| 5.8 | 4.50 | 4.48 | 4.45 | 4.43 |
| 6 | 4.66 | 4.63 | 4.60 | 4.57 |
| 6.2 | 4.81 | 4.77 | 4.74 | 4.70 |
| 6.4 | 4.94 | 4.88 | 4.86 | 4.79 |
| 6.6 | 5.04 | 4.95 | 4.95 | 4.86 |
| 6.8 | 5.11 | 4.99 | 5.01 | 4.89 |
| 7 | 5.14 | 4.98 | 5.05 | 4.89 |
| 7.2 | 5.13 | 4.94 | 5.05 | 4.86 |
| 7.4 | 5.09 | 4.87 | 5.03 | 4.81 |
| 7.6 | 5.02 | 4.78 | 4.99 | 4.75 |
| 7.8 | 4.93 | 4.67 | 4.93 | 4.67 |
| 8 | 4.83 | 4.56 | 4.86 | 4.59 |
| 8.2 | 4.72 | 4.44 | 4.79 | 4.50 |
| 8.4 | 4.61 | 4.32 | 4.70 | 4.41 |
| 8.6 | 4.50 | 4.21 | 4.62 | 4.33 |
| 8.8 | 4.39 | 4.10 | 4.53 | 4.24 |
| 9 | 4.28 | 3.99 | 4.44 | 4.14 |
| 9.2 | 4.18 | 3.88 | 4.35 | 4.05 |
| 9.4 | 4.07 | 3.77 | 4.26 | 3.96 |

| Log K _{ow} | Log BCF {1 mg DOC/L, H. azteca} | Log BCF {2 mg DOC/L, H. azteca} | Log BCF {1 mg DOC/L, fish} | Log BCF {2 mg DOC/L, fish} |
|---------------------|---------------------------------------|---------------------------------------|----------------------------------|----------------------------------|
| 9.6 | 3.96 | 3.66 | 4.16 | 3.86 |
| 9.8 | 3.86 | 3.56 | 4.06 | 3.76 |
| 10 | 3.75 | 3.45 | 3.97 | 3.67 |

Predictions were done for 5% body lipid content.